PA 1266198

THE UNITED STATES OF AMERICA

TO ALL TO WHOM THESE PRESENTS SHALL COME:

UNITED STATES DEPARTMENT OF COMMERCE

United States Patent and Trademark Office

December 30, 2004

THIS IS TO CERTIFY THAT ANNEXED HERETO IS A TRUE COPY FROM THE RECORDS OF THE UNITED STATES PATENT AND TRADEMARK OFFICE OF THOSE PAPERS OF THE BELOW IDENTIFIED PATENT APPLICATION THAT MET THE REQUIREMENTS TO BE GRANTED A FILING DATE UNDER 35 USC 111.

APPLICATION NUMBER: ***60/531,618***
FILING DATE: ***December 23, 2003***

By Authority of the
COMMISSIONER OF PATENTS AND TRADEMARKS

P. SWAIN
Certifying Officer

PTO/SB/16 (08-03)
Approved for use through 07/31/2006. OMB 0651-0032
U.S. Patent and Trademark Office: U.S. DEPARTMENT OF COMMERCE
Under the Paperwork Reduction Act of 1995, no persons are required to respond to a collection of information unless it displays a valid OMB control number

PROVISIONAL APPLICATION FOR PATENT COVER SHEET

This is a request for filing a PROVISIONAL APPLICATION FOR PATENT under 37 CFR 1.53(c).

Express Mail Label No.

INVENTOR(S)		
Given Name (first and middle [if any])	Family Name or Surname	Residence (City and either State or Foreign Country)
Van Suong	Hoa	Brossard, Canada
Weiping	Liu	Montreal, Canada

Additional inventors are being named on the 1 *separately numbered sheets attached hereto*

TITLE OF THE INVENTION (500 characters max)

Method and system for making high performances epoxies and high performances epoxies made therewith

Direct all correspondence to: **CORRESPONDENCE ADDRESS**

☑ Customer Number: 25545

OR

☐ Firm or Individual Name					
Address					
Address					
City		State		Zip	
Country		Telephone		Fax	

ENCLOSED APPLICATION PARTS *(check all that apply)*

☑ Specification *Number of Pages* 24 ☐ CD(s), Number

☑ Drawing(s) *Number of Sheets* 30 ☐ Other (specify)

☐ Application Data Sheet. See 37 CFR 1.76

METHOD OF PAYMENT OF FILING FEES FOR THIS PROVISIONAL APPLICATION FOR PATENT

☑ Applicant claims small entity status. See 37 CFR 1.27.

☐ A check or money order is enclosed to cover the filing fees.

☑ The Director is hereby authorized to charge filing fees or credit any overpayment to Deposit Account Number 07-1742

☐ Payment by credit card. Form PTO-2038 is attached.

FILING FEE Amount ($): 80.00

The invention was made by an agency of the United States Government or under a contract with an agency of the United States Government.

☑ No.

☐ Yes, the name of the U.S. Government agency and the Government contract number are:

Respectfully submitted,

SIGNATURE

TYPED or PRINTED NAME Jean H. Dubuc

TELEPHONE (514) 397-7607

Date December 23, 2003

REGISTRATION NO. 26,374 *(if appropriate)*

Docket Number GB/13234.30

USE ONLY FOR FILING A PROVISIONAL APPLICATION FOR PATENT

This collection of information is required by 37 CFR 1.51. The information is required to obtain or retain a benefit by the public which is to file (and by the USPTO to process) an application. Confidentiality is governed by 35 U.S.C. 122 and 37 CFR 1.14. This collection is estimated to take 8 hours to complete, including gathering, preparing, and submitting the completed application form to the USPTO. Time will vary depending upon the individual case. Any comments on the amount of time you require to complete this form and/or suggestions for reducing this burden, should be sent to the Chief Information Officer, U.S. Patent and Trademark Office, U.S. Department of Commerce, P.O. Box 1450, Alexandria, VA 22313-1450. DO NOT SEND FEES OR COMPLETED FORMS TO THIS ADDRESS. SEND TO: Mail Stop Provisional Application, Commissioner for Patents, P.O. Box 1450, Alexandria, VA 22313-1450

If you need assistance in completing the form, call 1-800-PTO-9199 and select option 2

PROVISIONAL APPLICATION COVER SHEET
Additional Pag

PTO/SB/16 (08-03)
Approved for use through 07/31/2006 OMB 0651-0032
U.S. Patent and Trademark Office; U S DEPARTMENT OF COMMERCE

Docket Number GB/13234 30

INVENTOR(S)/APPLICANT(S)

Given Name (first and middle [if any])	Family or Surname	Residence (City and either State or Foreign Country)
Maron	Pugh	Pointe Claire, Canada

Number 1 of 1

WARNING: Information on this form may become public. Credit card information should not be included on this form. Provide credit card information and authorization on PTO-2038.

TITLE OF THE INVENTION

Method and system for making high performances epoxies and high performances epoxies made therewith.

FIELD OF THE INVENTION

[0001] The present invention relates to epoxies. More specifically, the present invention is concerned with a method and a system for making high performances epoxies.

BACKGROUND OF THE INVENTION

[0002] Since most epoxy resins for use in high temperature structural applications are brittle, a considerable amount of work has been undertaken in an attempt to enhance the toughness of these materials, in particular for applications in the fields of aeroindustry, space industry and automobile industry, or even in such fields as sport equipment manufacturing, adhesive and sealant manufacturing and manufacturing of components for pipes, boats and reservoirs for example.

[0003] Typical toughening methods include the addition of a second phase such as rubber particles, thermoplastic particles or mineral fillers.

[0004] Polymer-layered silicate nanocomposites are another avenue, due to dramatic improvements in mechanical properties, barrier properties and thermal resistance at low clay loading observed in these materials as compared with a pristine matrix, i.e. with a polymer without clay.

[0005] It has been shown that organoclay may simultaneously

improve both toughness and elastic modulus of epoxy resins in a more efficient way than fillers. Therefore, nanocomposite technology using organoclay as a nano-scale reinforcement offers an interesting alternative for modifying epoxy resins. Clay minerals are principally silicates of aluminium, iron, and magnesium and belong to the phyllosilicate (or layer silicate) family of minerals. Epoxies are usually thermosetting resins made by polymerisation of an epoxide, such as ethylene oxide or epichlorohydrin, especially with a diphenol.

[0006] The United States patent US 4,465,797 by Brownscombe et al. describes a reinforced polymer composition comprising an epoxy resin matrix having intimately distributed therein a particulate or filamentary silicate or aluminosilicate mineral, in concentrations in the range from 10-30 phr (parts per hundred of resin by weight). A method for preparing such reinforced polymer composition comprises mixing the components into a liquid resin mixture, applying pressure thereto, forcing it through a ¾" diameter line into a mold, and removing the pressure. In US 5,840,796, Badescha et al. disclose a polymer nanocomposites comprising a mica-type layered silicate and having an exfoliated structure or an intercalated structure resulting from mechanical shear.

[0007] In European patent EP 0890616, Suzuki describes an epoxy composite comprising sheet-like clay reinforcement for improving the mechanical strength. In United States patent US 6,391,449, Lan et al. describe a method for fabricating polymer-clay intercalates exfoliates nanocomposites comprising preparing a mixture of at least two swellable matrix polymers and incorporating the mixture with a matrix polymer by melt processing the matrix polymer with the mixture. Barbee et al., in US patent US 6,384,121, contemplate producing a nanocomposite comprising an epoxy resin and layered clay material, by forming a concentrate of the clay material and melt

compounding the concentrate with the epoxy matrix. Polansky et al. in Us patent US 6,287,992 propose a polymer nanocomposite comprising an epoxy resin matrix having dispersed therein particles derived from a multilayered inorganic material, and having an increased fracture toughness and enhanced barrier properties against small molecules.

[0008] Lorah et al., in the published United states patent application US 2002/0055561, recently contemplated a method for producing improved epoxy nanocomposite characterised by a uniform dispersion of clay therein by enhancing the affinity between the clay and the polymer at the interface.

[0009] Layered silicate clay is seen as an ideal reinforcement for polymers due to its high aspect ratio, but untreated clay is not easily dispersed in most polymers because of its natural hydrophilicity and incompatibility with organic polymers.

[0010] The high-performance tetraglycidyl-4, 4'-diaminodiphenylmethane (TGDDM) epoxy resin and 4, 4'-diaminodiphenyl sulphone (DDS) system is widely used as the matrix for advanced composites in military and civil aircraft due to its good comprehensive properties such as excellent adhesion with fiber, relatively high strength and stiffness at room and elevated temperatures, processing versatility and reasonable cost etc. However, this resin system is very brittle and flammable, and has a high equilibrium content of water absorption.

[0011] A hybrid approach of adding both fillers and rubbers to epoxy resins has also been studied. However, a high concentration of fillers results in the reduction of processability.

[0012] Therefore there appears to be still a need in the art for an improved method and system for making high-performances epoxies.

SUMMARY OF THE INVENTION

[0013] There is provided a method for making a high performance epoxy comprising the steps of incorporating organoclay particles of a dimension in a nanometer range in a solution of a swelling agent to form an organoclay mixture; submitting the organoclay mixture to a shearing flow under a high pressure and a high velocity; submitting the organoclay mixture to a collapse of pressure; and mixing the organoclay mixture with an epoxy; whereby a fine and homogeneous distribution of particles of nano-dimensions in the epoxy is obtained.

[0014] Other objects, advantages and features of the present invention will become more apparent upon reading of the following non-restrictive description of embodiments thereof, given by way of example only with reference to the accompanying drawings.

BRIEF DESCRIPTION OF THE DRAWINGS

[0015] In the appended drawings:

[0016] Figure 1 is a flowchart of a method for making high performances epoxies;

[0017] Figure 2 is a schematic illustration of a system for making high performances epoxies;

[0018] Figure 3 shows optical micrographs of epoxy made by DMM a) containing 6-phr unmodified clay and b) containing 6-phr organoclay;

[0019] Figure 4 is a graph of an area percentage of agglomerates in nanocomposites and filler composites as a function of clay loading;

[0020] Figure 5 illustrates schematically the dispersion of organoclay and unmodified clay;

[0021] Figure 6 shows XRD patterns of unmodified clay and of composites thereof made with the DMM;

[0022] Figure 7 shows XRD patterns of I.30E organoclay and of nanocomposites thereof with the DMM;

[0023] Figure 8 shows XRD patterns of I.30 E and of nanocomposites thereof with the HPMM;

[0024] Figure 9 shows AFM micrographs of a) a DGEBA/BF_3.MEA epoxy system (1 x 1μm); b) a two-phase structure of a rubber-modified epoxy (30 x 30 μm); c) a two-phase structure of a rubber-modified epoxy (1 x 1μm); d) a rubber-modified nanocomposite at 3-phr clay loading (30 x 30 μm); e) a rubber-modified nanocomposite at 3-phr clay loading (1 x 1 μm); f) a rubber-modified nanocomposite at 6-phr clay loading (1 x 1μm);

[0025] Figure 10 illustrates the behaviour of the glass transition temperature (Tg) of nanocomposites and filler composites as a function of clay loading;

[0026] Figure 11 illustrates the behaviour of the glass transition temperature (Tg) of nanocomposites and filler composites as a function of clay loading;

[0027] Figure 12 shows a degree of cure of nanocomposites with clay loading as a function of clay loading;

[0028] Figure 13 is a graph of the storage modulus at 50 °C of nanocomposites and filler composites as a function of clay loading;

[0029] Figure 14 is a graph of the compressive yield strength of nanocomposite and filler composites as a function of clay loading;

[0030] Figure 15 shows typical compressive stress-strain curves of pristine resin and modified epoxies;

[0031] Figure 16 is a graph of the compressive modulus of nanocomposite and filler composites as a function of clay loading;

[0032] Figure 17 is a graph of the compressive yield strength of modified nanocomposites as a function of clay loading;

[0033] Figure 18 is a graph of the compressive modulus of modified nanocomposite as a function of clay loading;

[0034] Figure 19 is a graph of the ultimate strength of modified nanocomposites as a function of clay loading;

[0035] Figure 20 is a graph of the fracture strain of modified nanocomposites as a function of clay loading;

[0036] Figure 21 is a graph of the hardness of modified nanocomposites as a function of clay loading;

[0037] Figure 22 is a graph of the critical stress intensity factor (K_{1C}) of nanocomposites and filler composites as a function of clay loading;

[0038] Figure 23 is a graph of the critical stress intensity factor (K_{1C}) of modified nanocomposites as a function of clay loading;

[0039] Figure 24 is a graph of the critical strain energy release rate (G_{1C}) of nanocomposites and filler composites as a function of clay loading;

[0040] Figure 25 is a graph of the critical strain energy release rate (G_1c) of modified nanocomposites as a function of clay loading;

[0041] Figure 26 shows SEM micrographs of fracture surface of filler composites made with the DMM at 6-phr unmodified clay;

[0042] Figure 27 shows SEM micrographs of fracture surface of nanocomposites made with the DMM at 6-phr organoclay;

[0043] Figure 28 shows SEM micrographs of fracture surface of nanocomposites with the HPMM at 1.5-phr organoclay; and

[0044] Figure 29 shows SEM micrographs of a) a pristine resin

sample; b) modified epoxy at 20-phr CTBN rubber content; c) of a nanocomposite at 6-phr clay loading; d) of a nanocomposite at 6-phr clay loading (×10000); e) of an epoxy modified with both rubber and organoclay at low clay loading; f) of an epoxy modified with both rubber and organoclay at low clay loading at a high magnification image.

DESCRIPTION OF EMBODIMENTS OF THE INVENTION

[0045] Generally stated, the present invention provides a method and a system for making epoxies with improved mechanical properties.

[0046] As illustrated in Figure 1, a method according to the present invention comprises incorporating clay particles of a dimension in the nanometer range in a liquid solution of a swelling agent (step 110), submitting the mixture to high pressure and velocity yielding a shearing flow and to breaking impacts (step 120), then to a lower pressure (step 130); and then mixing the resulting clay mixture with an epoxy (step 140).

[0047] The step 110 comprises mixing a swelling agent with diluents and hardeners, and with clay particles, as will be described with more details hereinbelow in relation to specific examples.

[0048] The step 120 comprises submitting the mixture to a velocity yielding a shearing flow in a micrometer-range circuit allowing breaking impacts of the particles against walls thereof.

[0049] In step130, the particles explode into the mist of the liquid solution due to the smaller pressure.

[0050] In step 140, the resulting clay mixture is mixed with an epoxy and other ingredients and additives such as diluents and hardeners as is well known in the art, yielding an improved performance epoxy (step 140). The epoxy may be a rubber-modified epoxy, as will be shown further herein.

[0051] A system for achieving the above-described method may take a form illustrated in Figure 2. Such a system comprises an input 12 for the mixture of liquid and clay, a first section 14 where a pressure increases, leading to a second section 16 where the velocity increases sharply and where breaking impacts of the particles against walls thereof are favoured, and to a chamber 18 of collapse of the pressure. At an output 20, an extremely fine and homogeneous distribution of the particles of nano-dimensions is obtained.

[0052] In the case of a tubular structure, the first section 14 is typically by a small diameter of a tubular structure used, so that the mixture is submitted to a high pressure of the order of 20.000 psi (pounds per square inch) for example, and a high velocity, thereby allowing shearing in the liquid solution to occur in tubes of a diameter about 0.1 mm for example. The second section 16 may have a zig zag configuration for example, so as to increase a length of breaking impact occurrences.

[0053] The method described hereinabove, referred to hereinafter as HPPM, is used to fabricate organoclay nanocomposite and filler composite epoxies, using as a starting epoxy an epoxy resin such as TGDDM (N, N, N', N'-tetraglycidyl-4, 4'-diaminodiphenylmethane), with a hardener such as DDS (4, 4'-diaminodiphenyl sulphone); as an organoclay a commercially available organoclay suitable for dispersion into an epoxy resin such as Nanomer I.30E (Nanocor); and as an unmodified clay, a natural montmorillonite such as Cloisite Na^+ (Southern Clay Product).

[0054] The method described hereinabove is also used to fabricate rubber-modified epoxy nanocomposites using as a starting epoxy a DGEBA epoxy resin (a diglycidyl ether of bisphenol A), with a curing agent such as boron trifluoride monoethylamine (BF_3-MEA); as a rubber a reactive liquid rubber such as Hycar CTBN1300×8 (Noveon Inc.); and as an organoclay an octadeyl amine-modified montmorillonite suitable for dispersion into epoxy resin, for example.

[0055] In both cases, the resulting epoxies are compared with corresponding ones synthesized with a standard direct-mixing method as known in the art, referred to hereinafter as DMM. For that purpose, a number of tests is carried on the produced range of the epoxy nanocomposites (epoxy plus organoclay), filler composites (epoxy plus unmodified clay), and on the hybrid epoxy nanocomposites modified with rubber, synthesized by the standard DMM and by the method of the present invention.

[0056] A first series of physical measurements aims at studying the morphology of the different epoxies.

[0057] As may be seen in the scanning electronic microscopy of Figures 3a and 3b, the standard DMM yields cured systems of filler composites containing a large number of agglomerates of unmodified clay, most of them transparent and having a clear interface with the resin due to their crystal structure (Figure 3a), and nanocomposites also exhibiting a large number of agglomerates with an observed maximum diameter of about 20 μm, the size and quantity of these agglomerates being larger than in the filler composites at a similar clay loading (Figure 3b). However, the standard DMM does not result in obvious changes in size and quantity of agglomerates in nanocomposites when modifying parameters such as the stirring rate, temperature and time of

mixing, or curing parameters.

[0058] In the mixture of organoclay and TGDDM epoxy formed by this standard DMM, examined right after it is prepared in order to study the formation of agglomerates, agglomerates are observed under an optical microscope when the mixture is diluted with acetone, which are similar to those observed in the cured samples above. Such results indicate the agglomerates in the nanocomposites result from a poor dispersion.

[0059] In sharp contrast, in the paste of organoclay and acetone mixed by the method of the present invention, inspected with optical microscopy for comparison, the size and quantity of agglomerates observed is considerably lower. Most of the agglomerates are less than 1 μm and the maximum diameter observed is only between about 1 and 2 μm, which seems to indicate the method of the present invention achieves a breaking down thereof.

[0060] Area percentages of agglomerates in the nanocomposites and filler composites (composites made using natural clay) are shown in Figure 4. This figure shows the results from composites made by three different methods, including nanocomposites made by DMM, which is the method currently available in the art, nanocomposites made by the HPMM and filler composites (composites made using natural clay) made by DMM. The nanocomposites formed by the DMM (squares) have area of agglomerates about twice as large as the filler composites (triangles) at a similar clay loading. Such a result may suggest that the unmodified clay is submitted to one mechanism for reduction of the size of the agglomerates: breaking of the particle size; whereas the organoclay in DMM is subjected to two competing processes (Figure 5): break up, which tends to decrease the size of the

agglomerates, and intercalation by resin and hardener, which tends to increase the size thereof. In contrast, the materials formed by the present invention (HPMM) (rhomboids) have a reduced agglomerate area, which indicates an increased dispersion. Breaking of the particles has reduced the size of the agglomerates down to sufficient small size to produce this result.

[0061] Figure 6 presents XRD curves of unmodified clay and filler composites obtained by the standard DMM thereof at different clay loadings. For a clay powder without epoxy, a prominent peak corresponding to the basal spacing of the clay occurs at 1.22 nm. At lower clay loadings in an epoxy, this prominent peaks shift slightly and the basal spacing of composites with 3-phr clay and 6-phr clay increases from 1.22 nm to 1.56 nm and 1.57 nm respectively, which indicates that a small quantity of hardener or resin is forced into galleries of the clay. However, as the clay loading increases, the basal spacing of the clay in the filler composites falls back to the original value as that of pure clay.

[0062] Figure 7 shows XRD curves of organoclay and nanocomposites thereof obtained by the standard DMM. A prominent peak corresponding to the basal spacing of the organoclay is observed at 2.37 nm, whereas in the filler composites, the prominent peaks are mostly absent, which confirms the formation of exfoliated nanocomposites, while a few shoulders and small peaks in some of the curves indicate the presence of intercalated nanocomposites. Therefore, it appears that the organoclays in the nanocomposites made with the standard DMM are exfoliated or intercalated, and that they are not uniformly distributed in the epoxy resin since most of them are aggregated on the micro scale.

[0063] XRD curves of organoclay nanocomposites produced by the

method of the present invention presented in Figure 8 show that the basal spacing of the clay increases from 2.37 nm to 3.22 nm. There are no peaks in the XRD curves of the nanocomposites containing 1.5-phr and 3-phr I.30E, and their curves are similar to those of the TGDDM-DDS system. Therefore, the method of the present invention enhances the degree of exfoliation of organoclay and breaks up the agglomerates of organoclay.

[0064] In the case of the rubber modified epoxy nanocomposites, in a typical AFM (atomic force microscope) micrograph of a DGEBA/ BF_3.MEA epoxy system (1×1μm) (Figure 9a), a two–phase microstructure, consisting of a bright matrix and relatively dark interstitial regions, may be observed, with bright nodules of a size in the range between 100 nm and 200 nm. When observing the two-phase structure of rubber-modified epoxy (Figures 9b and 9c), the rubber spheres being dispersed in the continuous epoxy matrix, it appears that the size of nodules in the rubber phase is larger than that in the epoxy phase and the interface between rubber and epoxy is indistinct.

[0065] The rubber particles of the hybrid nanocomposites at 3-phr clay loading may also observed (Figures 9d and 9e), wherein the nodules of rubber phase seem oriented and the interface is clear. On increasing the clay loading to 6-phr, a two-phase system of this hybrid nanocomposite is confirmed from Dynamic Mechanical Analysis (DMA) results (Figure 9f).

[0066] DMA is further used to measure the glass transition temperature (Tg) of the resulting epoxies.

[0067] In the case of the nanocomposites and filler composites, as may be observed in Figure 10, the glass transition temperature of nanocomposites made with the standard DMM (squares) appears to decrease

slightly when the clay loading increases, in contrast to that of the filler composites (triangles). Such a decrease is found to be of the order of 10 °C for the nanocomposite at 12-phr organoclay loading. In contrast, the Tg of nanocomposites made with the method of the present invention (rhomboids) appears to decrease very little and is higher than that made with the standard DMM (squares) at a similar clay loading. Such a reduction of Tg may be explained by the fact that the organoclay catalyzes the homopolymerization of the TGDDM resin during the mixing stage and hence modifies the network of the cured epoxy. Surface modifiers or small molecules from thermal degradation of the surface modifier at high temperature may exist in the system and act as lubricators.

[0068] Figure 11 shows the glass transition temperature (Tg) of the nanocomposites with (squares) and without CTBN (rhomboids). The nanocomposites without CTBN (rhomboids) have higher Tgs, but the Tg decreases slightly as a function of the clay loading. The reduction in Tg is found to be of the order of 10 °C for the nanocomposite at 6-phr organoclay loading. On the other hand, the nanocomposites with CTBN (squares) have lower Tgs due to the presence of CTBN, but the Tg increases with increasing the clay loading below 4.5-phr. The maximum enhancement is 21 °C at 4.5-phr clay loading. The changes of degree of cure for nanocomposites seem similar to those of Tg (shown in Figure 12). This indicates that adding organoclay into the pristine epoxy reduces the degree of cure, and thus Tg; conversely, adding organoclay into rubber-modified epoxies increases the degree of cure and Tg.

[0069] As may be seen in Figure 13, the storage modulus at 50°C of the nanocomposites and filler composites increases with increasing clay loading. However the increase for the nanocomposites (squares and triangles) is greater than for the filler composites (rhomboids).

[0070] Figures 14 and 16 show the compressive yield strength and compressive modulus of nanocomposites and filler composites, while Figures 15, 17-19 show typical compressive stress-strain curves of pristine resin and different modified epoxies (Figure 15), the compressive yield strength (Figure 17), the compressive modulus (Figure 18) and the ultimate strength (Figure 19) of the rubber modified nanocomposites respectively, as a function of the clay loading.

[0071] In Figure 14, both nanocomposites (square) and filler composites (triangles) show a compressive yield strength practically unchanged with different amounts of clay loadings. At lower clay loading, less than 3-phr and 6-phr respectively for filler composites and nanocomposites, the strength increases, but it decreases with increasing the clay loading above this value. The nanocomposites (triangles) even have slightly lower yield strength than filler composites (squares). However the modulus increase of nanocomposites (squares) is substantially higher than those of filler composites (triangles) (Figure 16). There is more than 20% increase in modulus of TGDDM-DDS at 9-phr organoclay loading but only a 10% increase for untreated clay.

[0072] In Figure 15, all curves show apparent ductility with different modulus, ultimate strength, yield strength and fracture strain. The pristine resin has a higher yield strength but the lowest fracture strain. The nanocomposite without CTBN has the highest modulus, ultimate strength and yield strength. By adding CTBN into epoxy resin, fracture strain increases, but yield strength, modulus and ultimate strength are reduced. Furthermore, by adding organoclay into the rubber-modified epoxy, the strength in the plastic region is increased whilst maintaining the high fracture strain.

[0073] The yield strength, modulus, ultimate strength of modified epoxies as a function of the clay loading are shown in Fig 17-19 respectively. For the nanocomposites without CTBN, all these compressive properties increase with increasing the clay loading. They show 25.1 %, 29.1%, and 5.8% increases respectively, compared to pristine resin with 6-phr organoclay loading. On the other hand, for the nanocomposite with CTBN, the yield strength and ultimate strength also increased with increasing clay loading, but modulus and fracture strain were almost unchanged. The hybrid nanocomposite with 20-phr CTBN and 6-phr organoclay shows 3.9%, 12.0% and 32.2% increases respectively, in modulus ultimate strength and yield strength, compared to with the rubber-modified epoxy at the same CTBN content.

[0074] Figure 20 further shows fracture strain of these rubber-modified nanocomposites as a function of clay loading. For the nanocomposites without CTBN, this compressive property shows an 9.6% increase compared to pristine resin with 6-phr organoclay loading, and for the nanocomposite with CTBN, like the modulus, the fracture strain is almost unchanged. The hybrid nanocomposite with 20-phr CTBN and 6-phr organoclay shows a 2.4% increase in the fracture strain, compared to with the rubber-modified epoxy at the same CTBN content.

[0075] The hardness of nanocomposites with and without CTBN is further shown in Figure 21. The nanocomposites without CTBN have higher hardness values but less improvement with increasing clay loading compared to the nanocomposites with CTBN. On adding 20-phr CTBN into the epoxy, the material lost about 15% in hardness, but it retrieved 11% after adding 6-phr organoclay into the rubber-modified epoxy.

[0076] In relation to fracture toughness, as known in the art, a critical stress intensity factor K_{1C} may be calculated from the following relation (in units of $MPa.m^{1/2}$):

$$K_{1C} = \sqrt{1000} \bullet \left(\frac{P_{max}}{BW^{1/2}} \right) f(x)$$

where: $x = a/W$ and P_{max} is a maximum load, B is a sample thickness, W is a sample width, a is a crack length.

[0077] A critical strain energy release rate G_{1C} may further be calculated from the following formula (in units of J/m^2):

$$G_{1C} = U/BW\Phi(x)$$

where

$$U = 1/2 P_{max} (u_{max} - u_i)$$

and P_{max} is a maximum load, B is a beam length, W is a beam width, u_{max} is a maximum displacement, u_i is an indentation displacement.

[0078] Figures 22 and 23 show the critical stress intensity factor K_{1C} of the nanocomposites and filler composites, and of the rubber epoxies respectively, as a function of clay loading, as measured by single-edge-notch bending (SENB). Figures 24 and 25 show the critical strain energy release rate G_{1C} of the nanocomposites and filler composites, and of the rubber epoxies respectively, as a function of clay loading, as measured by SENB.

[0079] The nanocomposites made with the standard DMM show an increase in both K_{1c} (Figure 22) and G_{1c} (Figure 24) higher than the filler composites as a function of clay loading. It shows more than 79% and 151% increase respectively, in K_{1c} and G_{1c} of TGDDM-DDS with12-phr organoclay loading but only a 36% and 66% increase for untreated clay.

[0080] The nanocomposites made with the method of the present invention shows a dramatic increase in fracture toughness at very low clay loading, with an increase in K_{1c} and G_{1c} 2 and 3 times respectively, at only 1.5-phr (about 1 wt %) organoclay loading.

[0081] In the case of the CTBN-modified nanocomposites, as compared to the nanocomposites without rubber, they show a further increase in both K_{1c} (Figure 23) and G_{1c} (Figure 25) (over the rubber-modified epoxies) as the clay loading increases. All the nanocomposites contain the same content of CTBN (20-phr) but with different organoclay contents ranging from 0 to 6-phr. At clay loading of less than 3-phr, fracture toughness increases slowly. But, beyond this value, there is a dramatic improvement in fracture toughness. K_{1c} and G_{1c} are increased by 2.2 and 7.6 times respectively, at 6-phr organoclay loading and 20-phr CTBN compared with the pristine epoxy system. Therefore, there is a superposition effect on fracture toughness of the hybrid epoxy nanocomposites modified with rubber and organoclay.

[0082] Scanning electron microscopy (SEM) is used to observe the toughening in the filler composites and nanocomposites. The pristine resin samples show smooth and featureless surfaces representing brittle failure in a homogenous material and even at high magnification. In a typical fracture topology of filler composites (6-phr clay loading), agglomerates may be observed in different sizes and a maximum diameter thereof is about 20 μm

(see Figures 26). The particles are debonded from the resin and voids are formed around the particles due to the poor compatibility and the low adhesive strength of interface between the epoxy and the untreated clay. Thus the toughness improvement may be attributed to crack tip blunting from these features. A small number of shallow 'river-markings' around the particles running in the direction of crack propagation is observed. These river-markings occurred as a result of crack deflection and subsequent propagation on two slightly different fracture planes. Nanocomposites made with the standard DMM exhibit very different fracture surfaces (Figure 27). Agglomerates are also visible and the maximum diameter is about 30 μm for these nanocomposites which is larger than that in the filler composites. But only a few parts of the interfaces are debonded form the resin and fewer voids are formed. This is attributed to the fact that the epoxy molecules intercalated the organoclay resulting in the formation of rigid, impenetrable and well-bonded agglomerates. These particles impeded the propagation of cracks. As a propagating crack became temporarily pinned and started to bow out between the particles, forming secondary cracks, more and deeper river-markings around agglomerates were formed. Therefore, in contrast to filler composites, the pinning effect may be more dominant than the crack tip blunting effect in enhancing the fracture toughness of nanocomposites with the standard DMM.

[0083] In a fracture surface of nanocomposites synthetized with the present method (Figure 28), no distinct agglomerates may be seen, even at relatively high magnification. Crack bifurcation may be observed at higher magnification and associated with the presence of very small particles of the dispersed clay that are assumed to be the pinning effect. Clearly, the incorporation and progressively better dispersion of the clay in the resin enhances the efficiency of this pinning effect and thus results in a considerable change in fracture behavior of this resin.

[0084] The fracture surface of a modified epoxy at 20-phr CTBN rubber content may also be observed using SEM (Figure 29). A two-phase microstructure with the rubber spheres dispersed in the continuous epoxy phase, is seen. Tearing of the material between two crack planes (see the white lines on figure 29b) may cause a surface step. There are some cavities observed in the rubber particles and the epoxy resin because of the cohesive failure of rubber particles. In figure 29c, the fracture surface of a nanocomposite at 6-phr clay loading exhibits very different failure mode and it looks like that of filler-modified epoxies). But, there are no distinct agglomerates observed even at relatively high magnification (×10000). The crack bifurcation is quite evident at such higher magnification in Figure 29d and this is associated with the presence of very small particles that are assumed to be the dispersed clay. Therefore, the toughening mechanisms of rubber and organoclay are different. When the epoxy was modified with both rubber and organoclay at low clay loading, the fracture surfaces show both features of fracture surfaces described above (Figure 29e). In a high magnification image (Figure 29f), the crack bifurcations are smaller. It indicates that the toughening by rubber dominated the toughness of this material at lower clay loading. On increasing the clay loading to 6-phr, the fracture surfaces exhibit a strong three-dimension appearance (Figure 29g and 29h). The rubber particles are not found, but the crack bifurcation is very strong. The cracks bifurcate creating multiple fracture surfaces and causing greater energy dissipation.

[0085] In summary, the standard DMM allows to synthetize nanocomposites in which the organoclay is exfoliated and/or intercalated as observed from XRD data, but does not achieve a uniform distribution thereof in the epoxy resin since it is mostly aggregated on a micro scale. Therefore, the nanocomposites made with the standard DMM show a higher toughness and modulus than filler composites, and a glass transition temperature (Tg) that

decreases slightly as the content of clay increases.

[0086] In sharp contrast, the method of the present invention enhances the degree of exfoliation of organoclay and breaks up the agglomerates of organoclay. As a result, the nanocomposites made with the method of the present invention show a dramatic improvement in fracture toughness at very low clay loading; that is, K_{1C} and G_{1C} are increased by 2 and 3 times respectively at 1.5-phr (about 1 wt%) organoclay loading over the pristine resin properties.

[0087] In the case of rubber-modified epoxies, the present method further improves on the fact that organoclay enhances Tg and mechanical performances. Modification with organocaly simultaneously improves the fracture toughness and compressive properties of DGEBA/ BF_3.MEA, that is, K_{1C} and G_{1C}, increased by 1.84 and 2.97 times, respectively; compressive modulus, ultimate strength, yield strength and fracture strain increased by 25.1 %, 29.1%, 5.8% and 9.6% respectively, at 6-phr concentration of CTBN, modification of the epoxy with organoclay and rubber not only further improves fracture toughness, that is, K_{1C} and G_{1C} are increased by 2.2 and 7.6 times respectively, at 6-phr organoclay loading and 20-phr CTBN compared to the pristine resin, but also enhances Tg, yield strength and ultimate strength compared with the rubber-modified epoxy with the same content of CTBN.

[0088] In relation to hybrid epoxy nanocomposites modified with organoclay and rubber people in the art are aware that they form most complicated systems, whose performance strongly depends on its morphology including dispersion and exfoliation of organoclay, degree of rubber phase separation, and degree of cure. Dispersion methods and cure parameters are found to have a high influence on the morphology.

[0089] The method and system of the present invention allows synthesizing nanocomposite epoxies wherein organoclay agglomerates are broken down with an increased degree of exfoliation of organoclay and increasingly dispersed. The Tg of nanocomposites made with the method of the present invention is increased and increasingly stable, while the compressive properties are dramatically increased at similar clay loading.

[0090] From the foregoing, it is now apparent that the present invention provides a method and a system allowing to fabricate epoxies having a fracture toughness many times higher than that of current epoxies, and enhanced barrier properties against small molecules, while produced at a cost similar to that of existing epoxies. As people in the art will appreciate, this increased fracture toughness improves greatly the capability of the material to absorb energy, for example form impact, and to resist growth of cracks.

[0091] Although the present invention has been described hereinabove by way of embodiments thereof, it can be modified, without departing from the spirit and nature of the subject invention as described herein.

WHAT IS CLAIMED IS:

1. A method for making a high performance epoxy as described herein.
2. A system for making a high performance epoxy as described herein.

ABSTRACT OF THE DISCLOSURE

A method comprising submitting a mixture of organoclay particles first to a high pressure and high velocity flow in a channel of micrometer range diameter which allows shearing of the particules in the mixture of organoclay particles, and then to a sudden lower pressure, whereby the particles explode into the mist of the mixture of organoclay particles, and mixing the resulting mixture of organoclay particles with a pristine epoxy, yielding an extremely fine and homogeneous distribution of the particles of nano-dimensions in the epoxy, yielding high-performance nanocomposite epoxy.

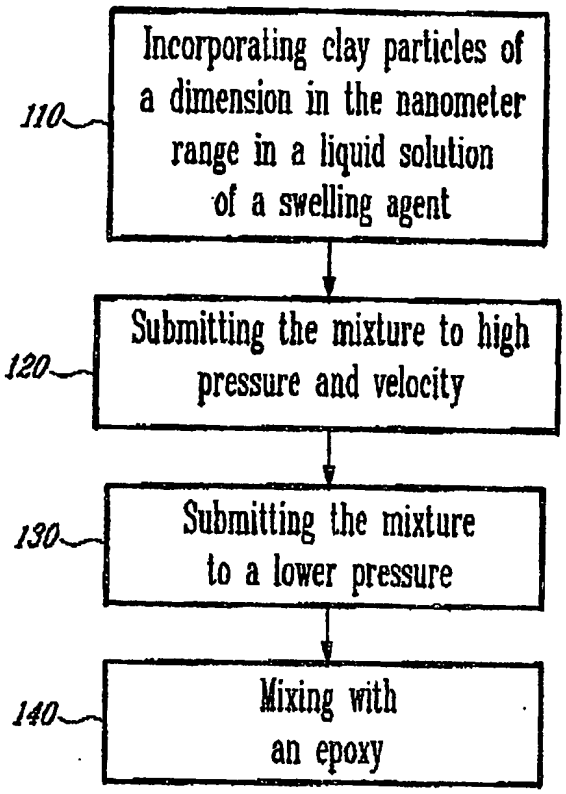

Fig. 1

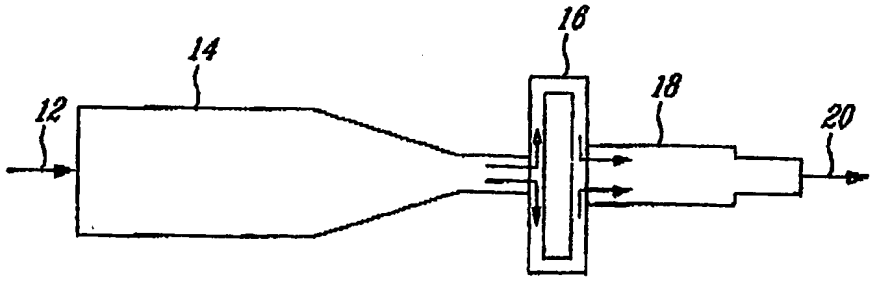

Fig. 2

Figure 3

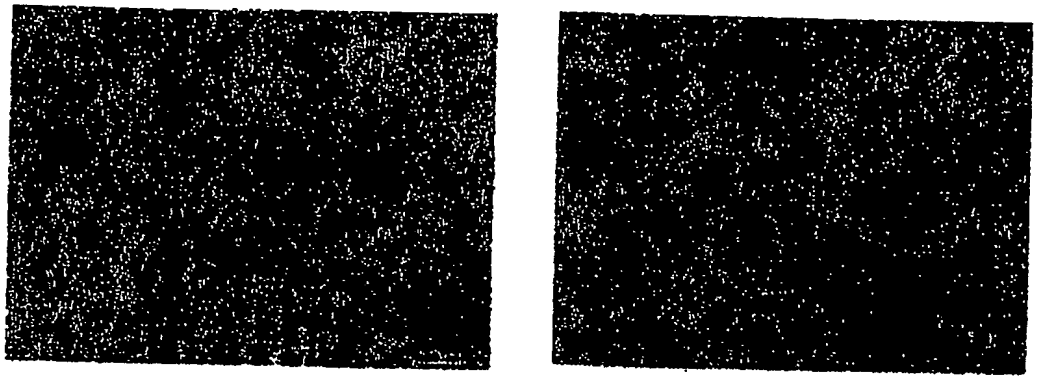

(a) (b)

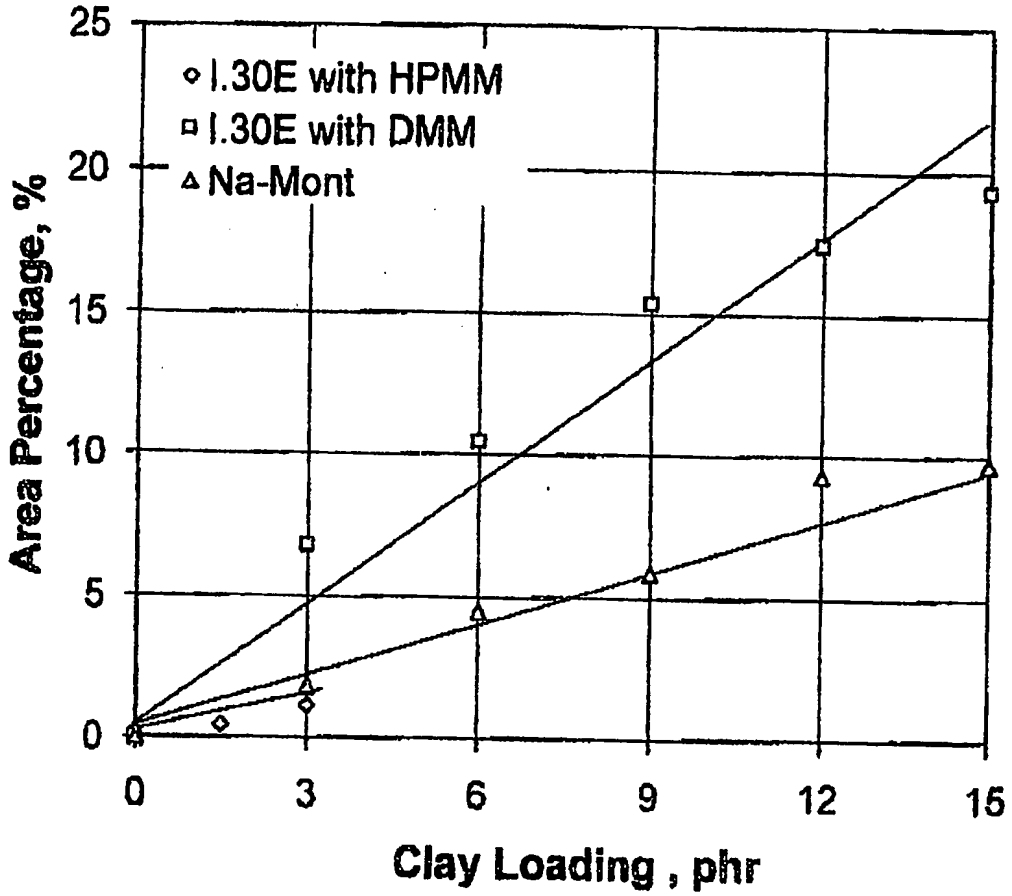

Fig. 4

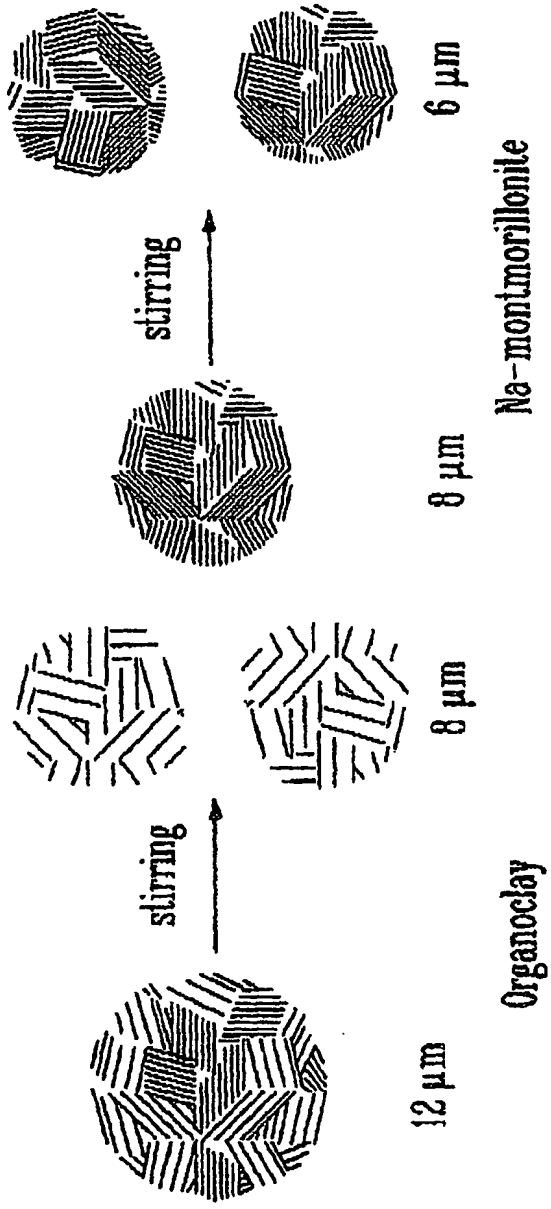

FIG. 5

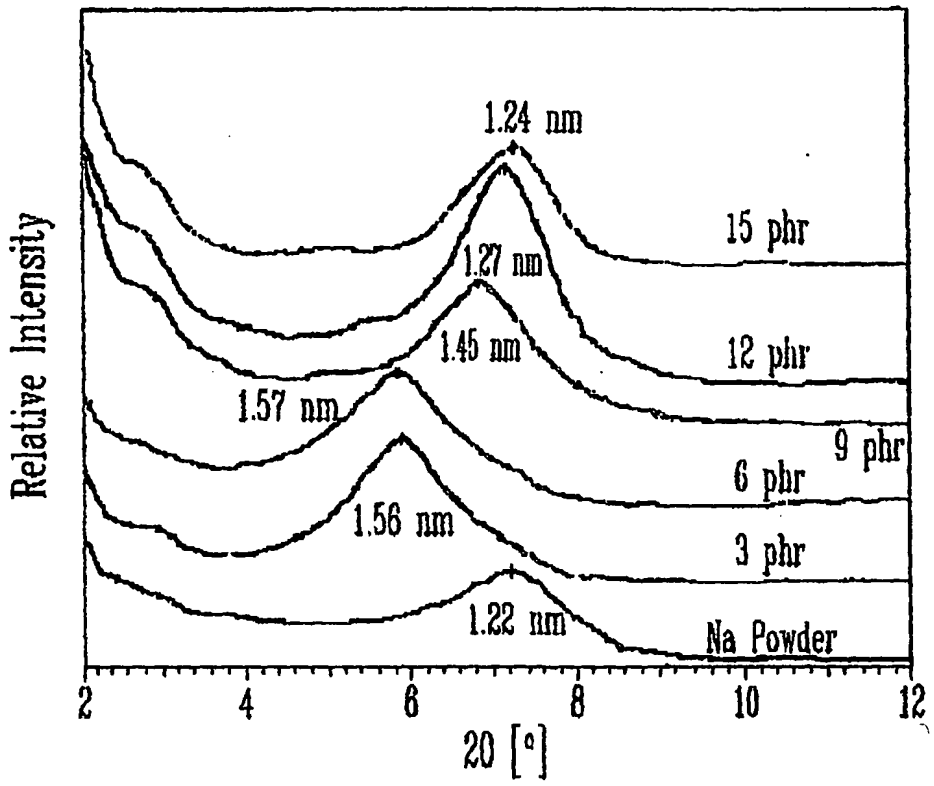

Fig. 6

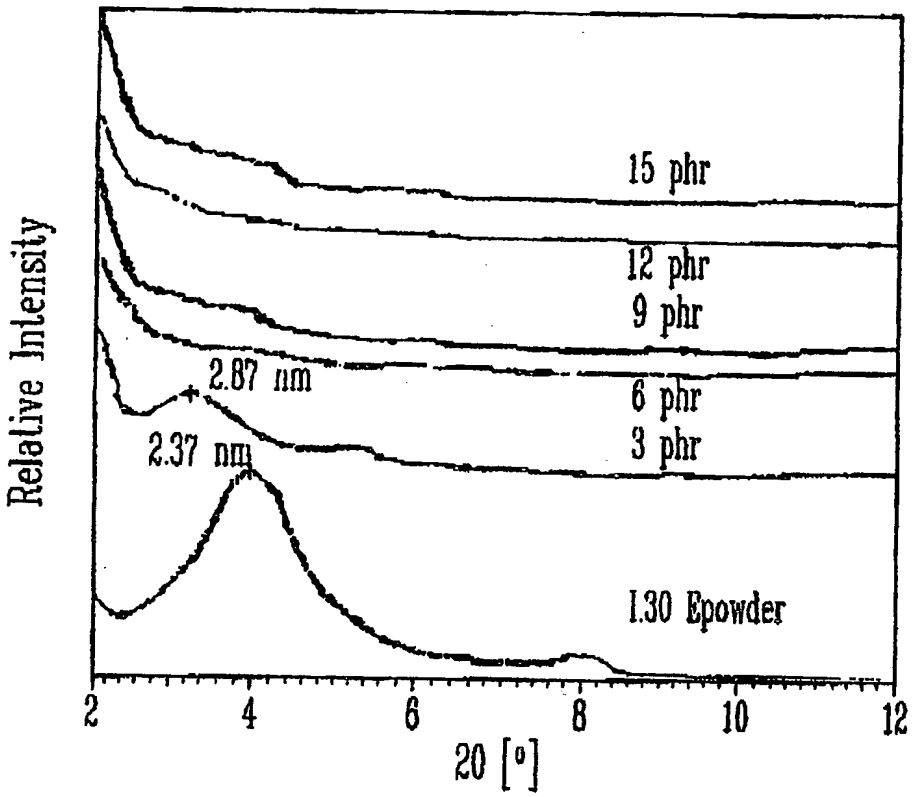
Relative Intensity
15 phr
12 phr
9 phr
6 phr
3 phr
I.30 Epowder
2.87 nm
2.37 nm
2
4
6
8
10
12
2θ [°]

FIG. 7

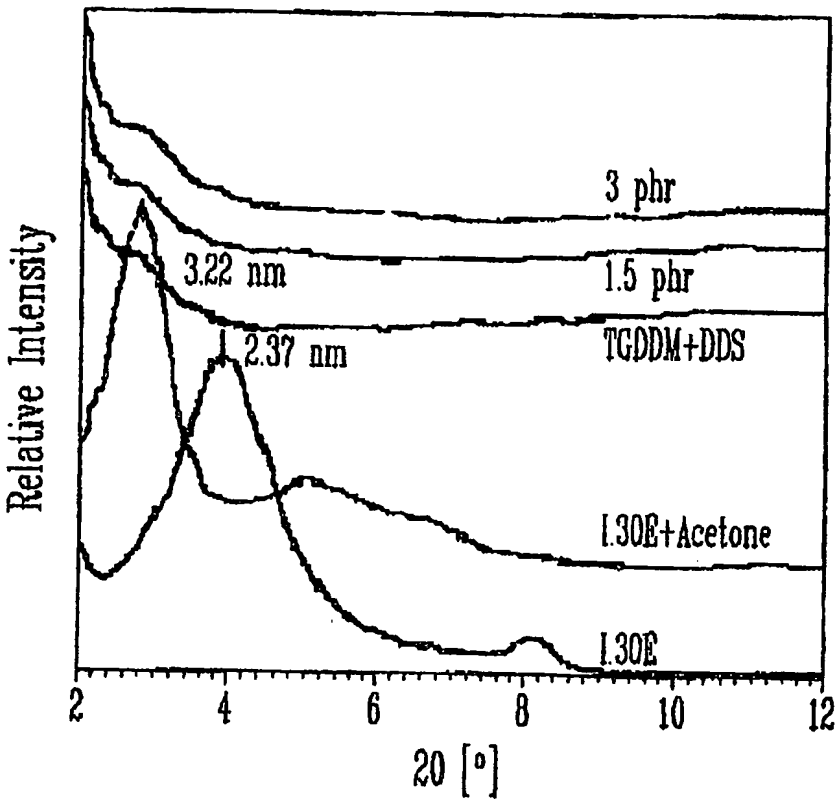
3 phr
1.5 phr
TGDDM+DDS
I.30E+Acetone
I.30E
3.22 nm
2.37 nm
Relative Intensity
2
4
6
8
10
12
2θ [°]

Fig. 8

Figure 9

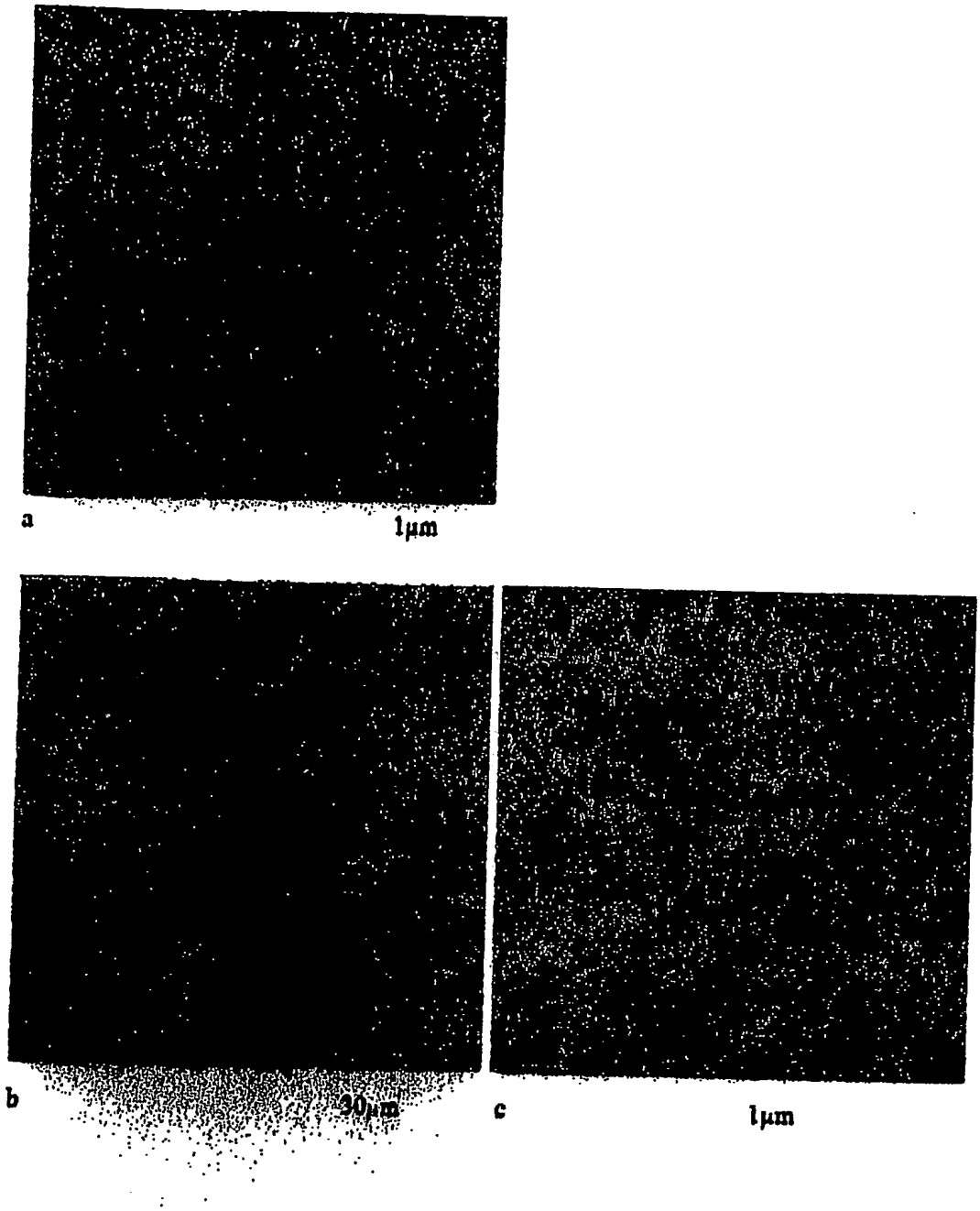

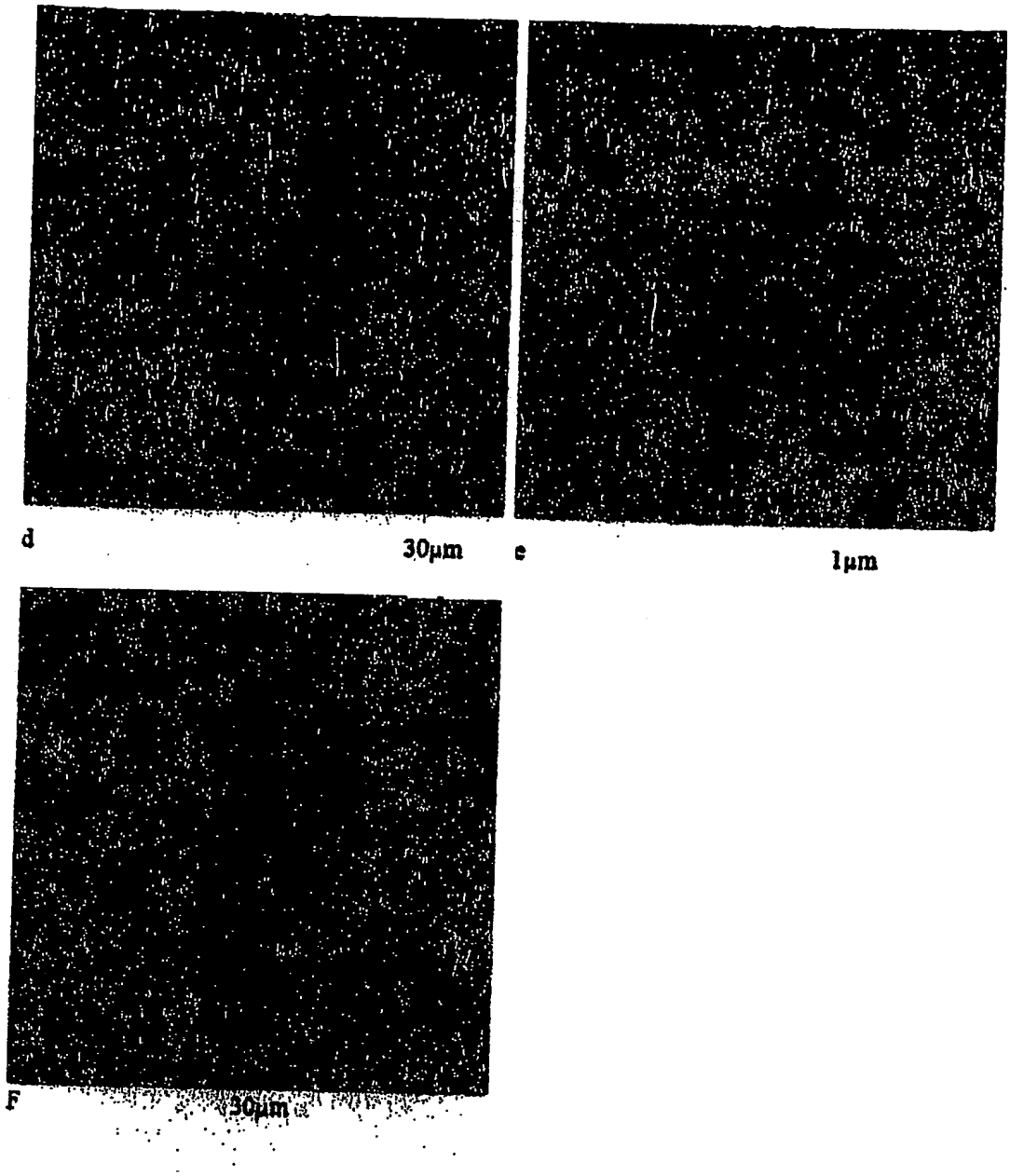

Figure 9

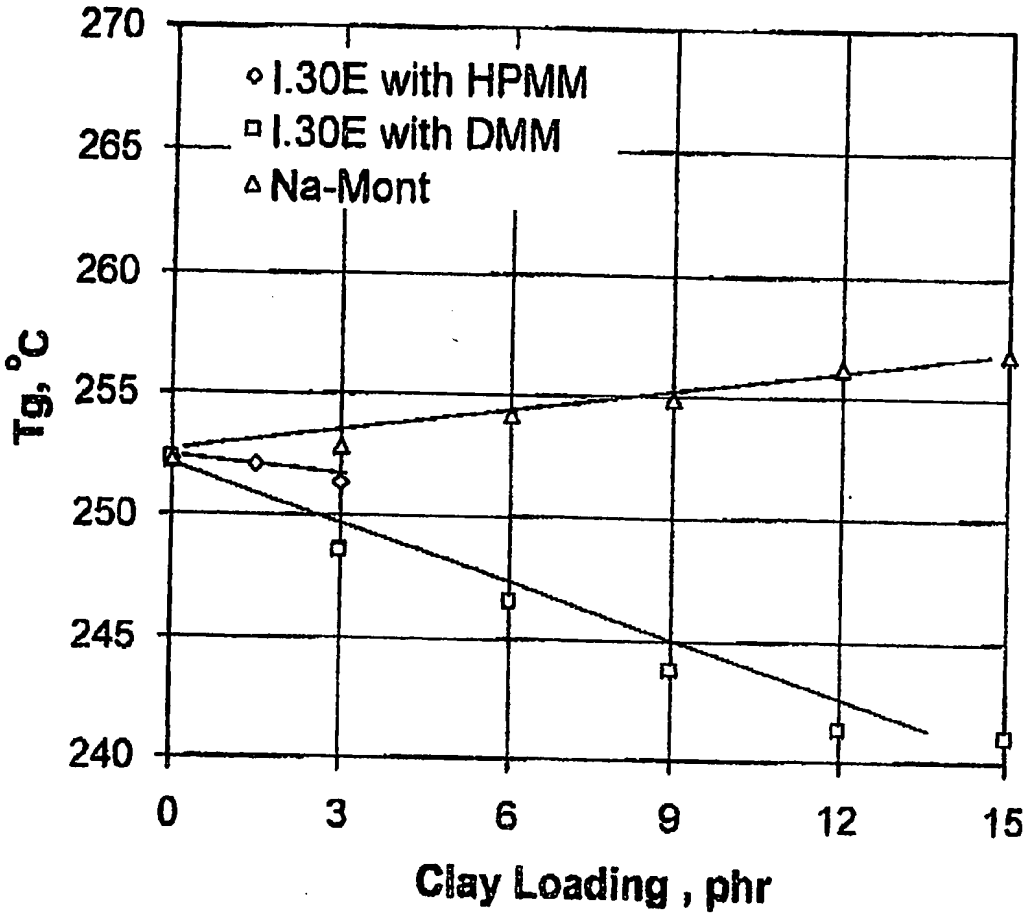
270
265
260
255
250
245
240
Tg, °C
I.30E with HPMM
I.30E with DMM
Na-Mont
0
3
6
9
12
15
Clay Loading , phr

Fig. 10

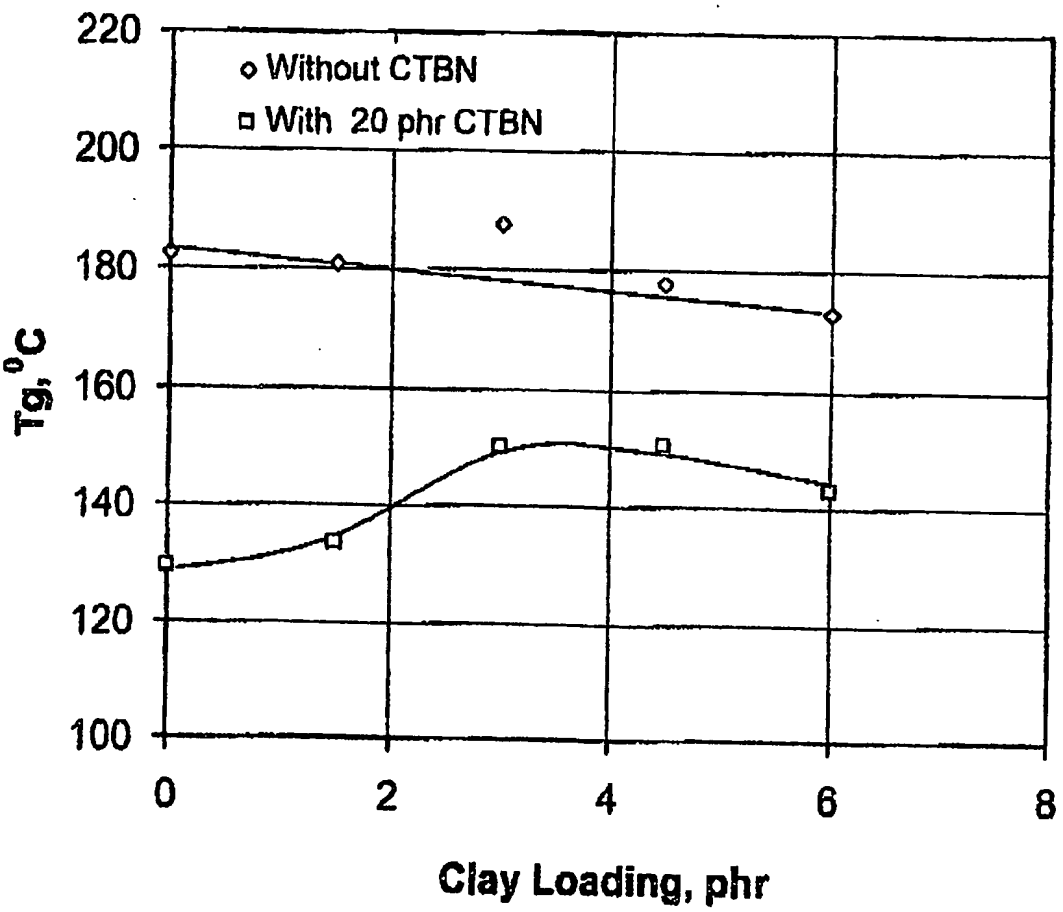

Fig. 11

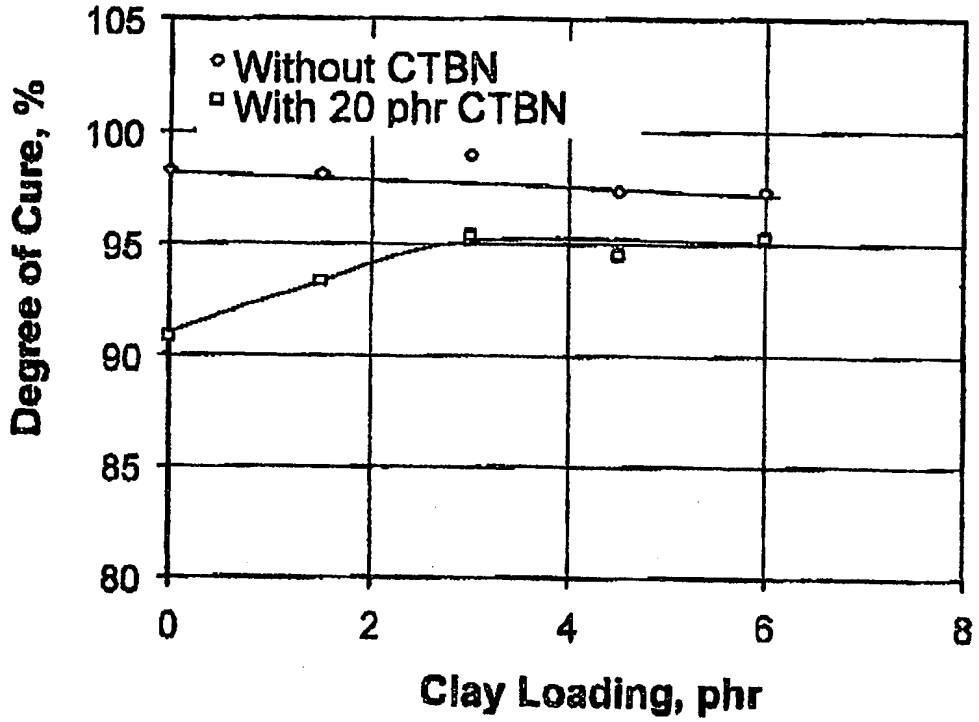
105
100
95
90
85
80
Degree of Cure, %
Without CTBN
With 20 phr CTBN
0
2
4
6
8
Clay Loading, phr

Fig. 12

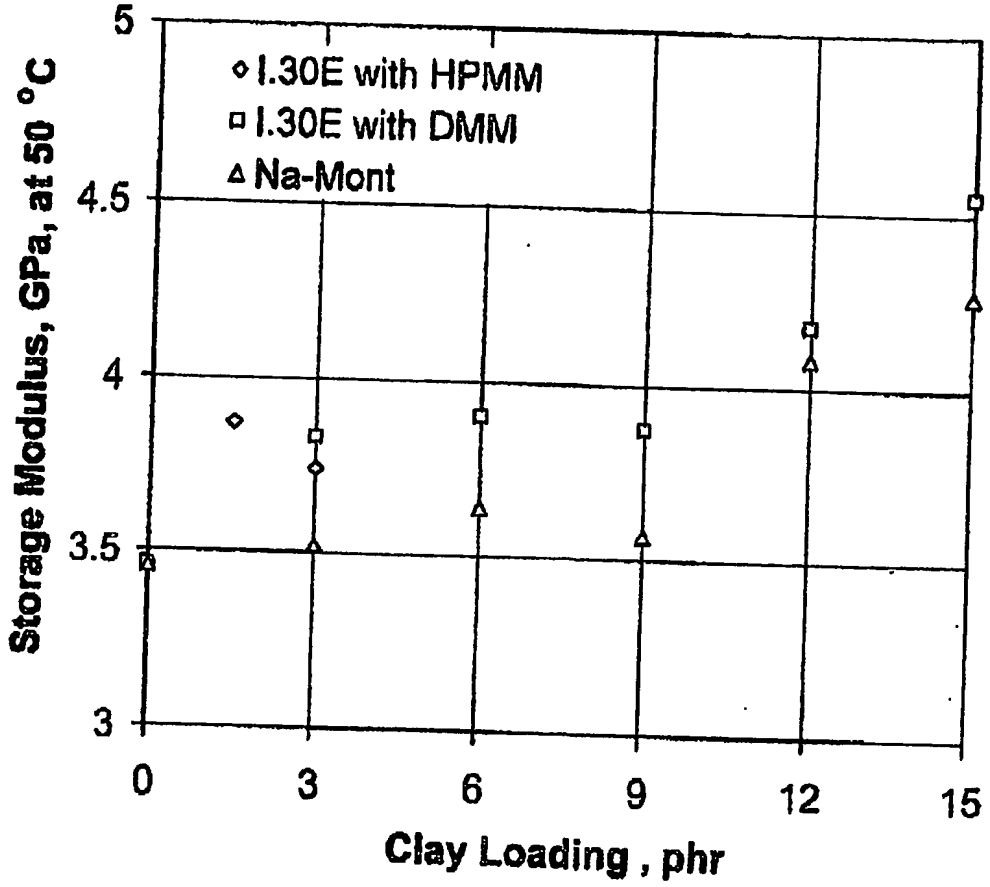
I.30E with HPMM
I.30E with DMM
Na-Mont
Storage Modulus, GPa, at 50 °C
5
4.5
4
3.5
3
0
3
6
9
12
15
Clay Loading , phr

Fig. 13

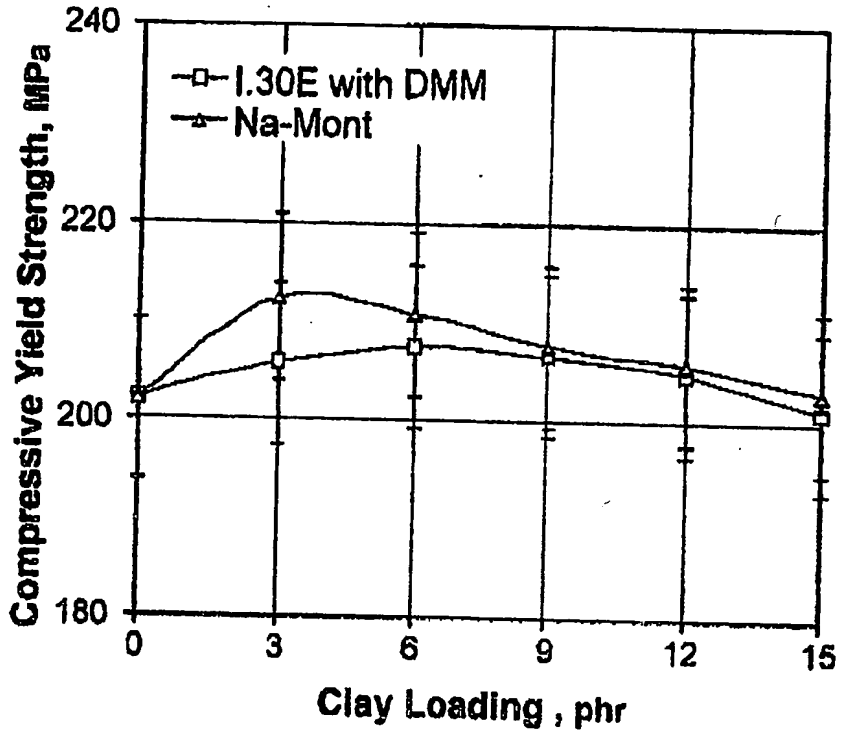
240
220
200
180
0
3
6
9
12
15
I.30E with DMM
Na-Mont
Compressive Yield Strength, MPa
Clay Loading , phr

FIG. 14

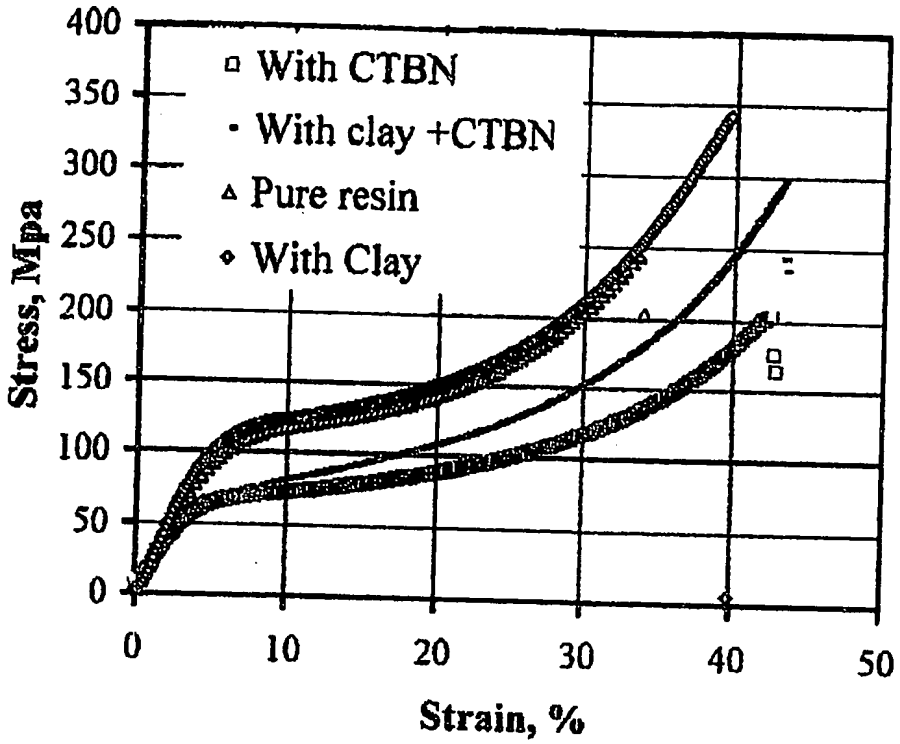
With CTBN
With clay +CTBN
Pure resin
With Clay
Stress, Mpa
Strain, %
400
350
300
250
200
150
100
50
0
0
10
20
30
40
50

Fig. 15

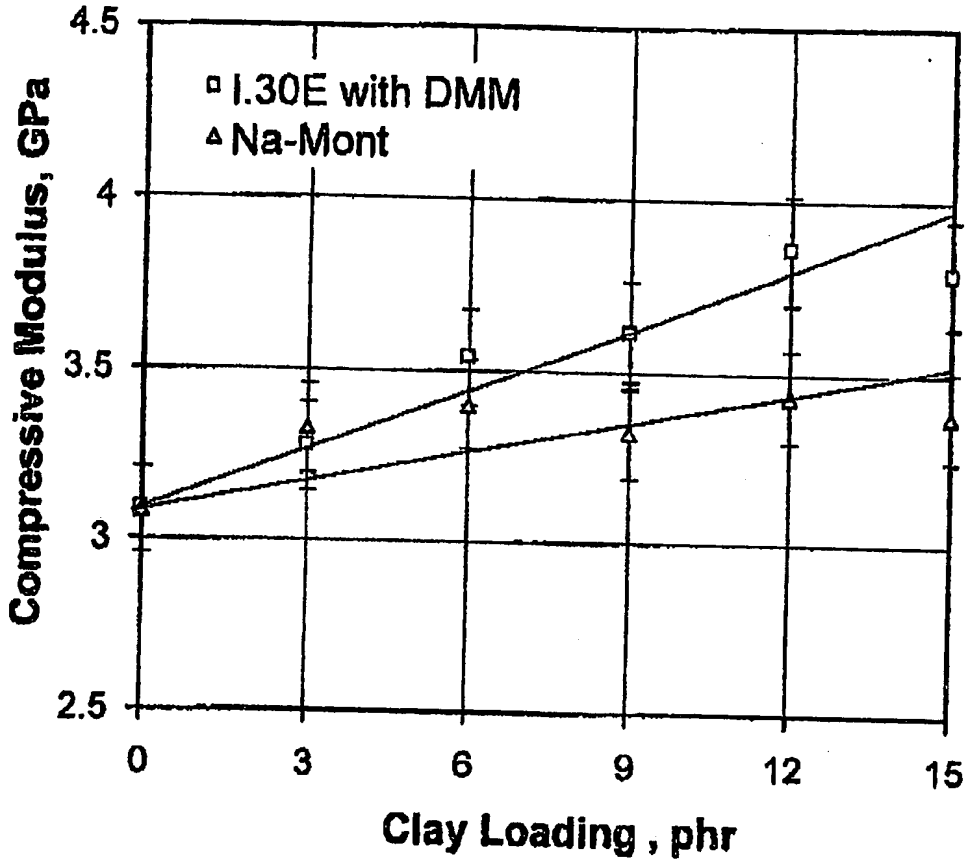
4.5
4
3.5
3
2.5
I.30E with DMM
Na-Mont
Compressive Modulus, GPa
0
3
6
9
12
15
Clay Loading , phr

FIG. 16

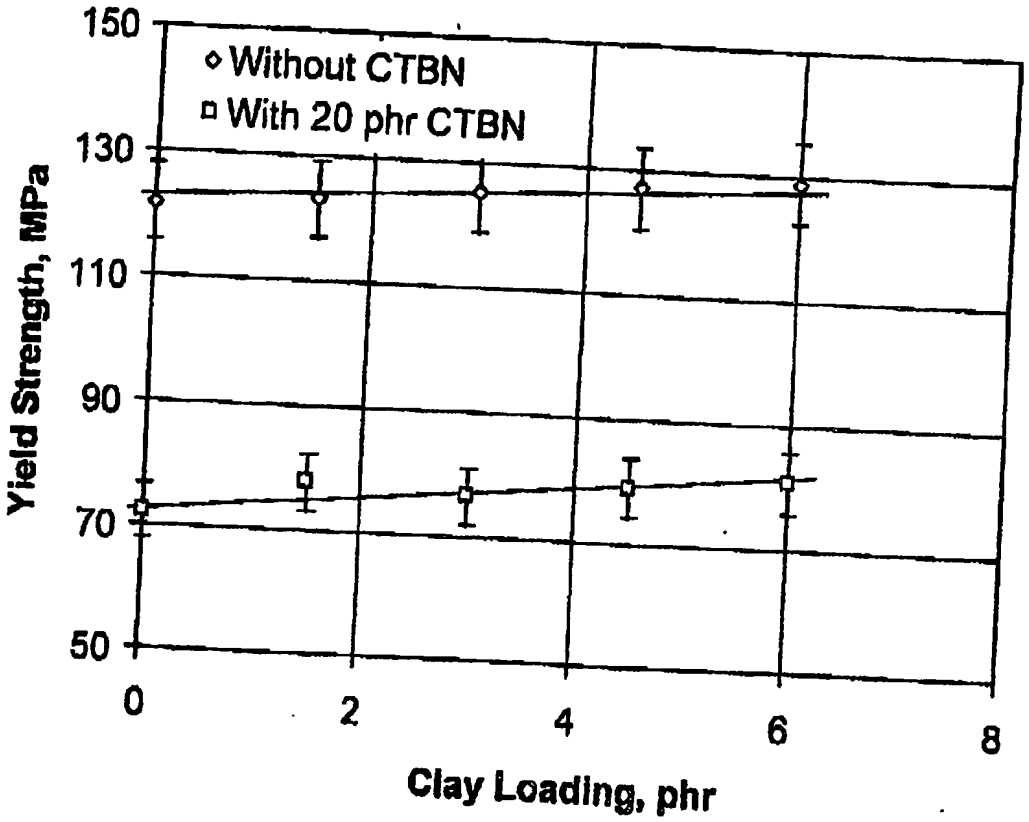
150
130
110
90
70
50
Without CTBN
With 20 phr CTBN
Yield Strength, MPa
0
2
4
6
8
Clay Loading, phr

FIG. 17

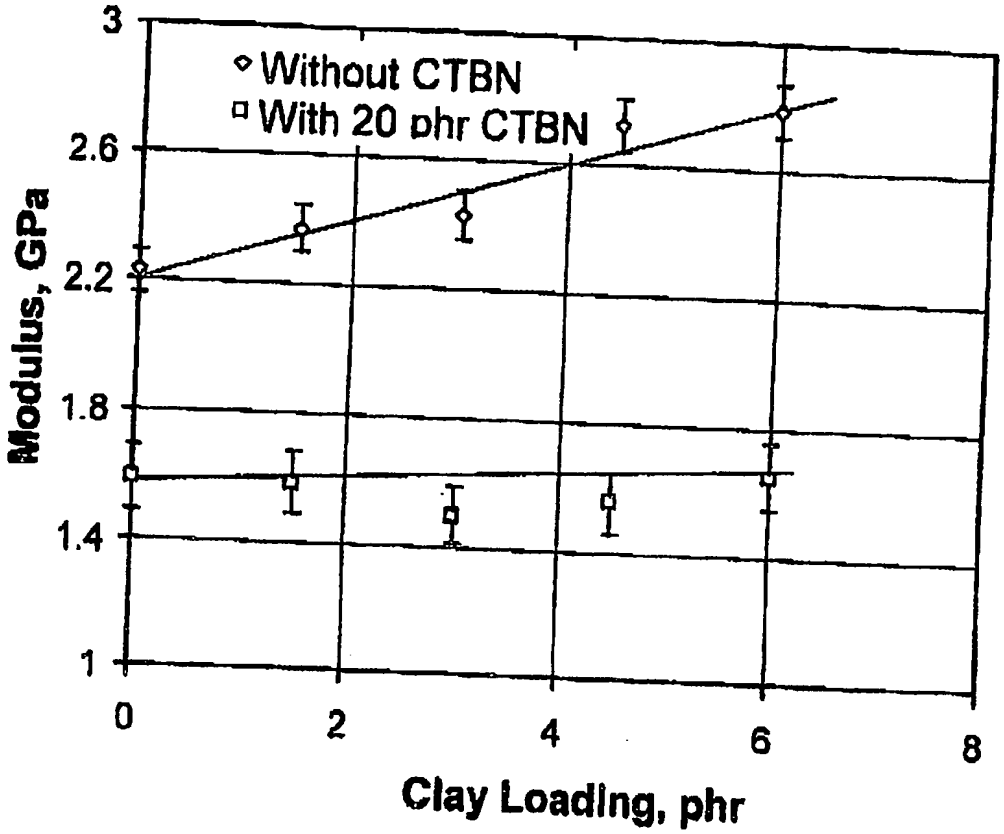
Without CTBN
With 20 phr CTBN
Modulus, GPa
3
2.6
2.2
1.8
1.4
1
0
2
4
6
8
Clay Loading, phr

Fig. 18

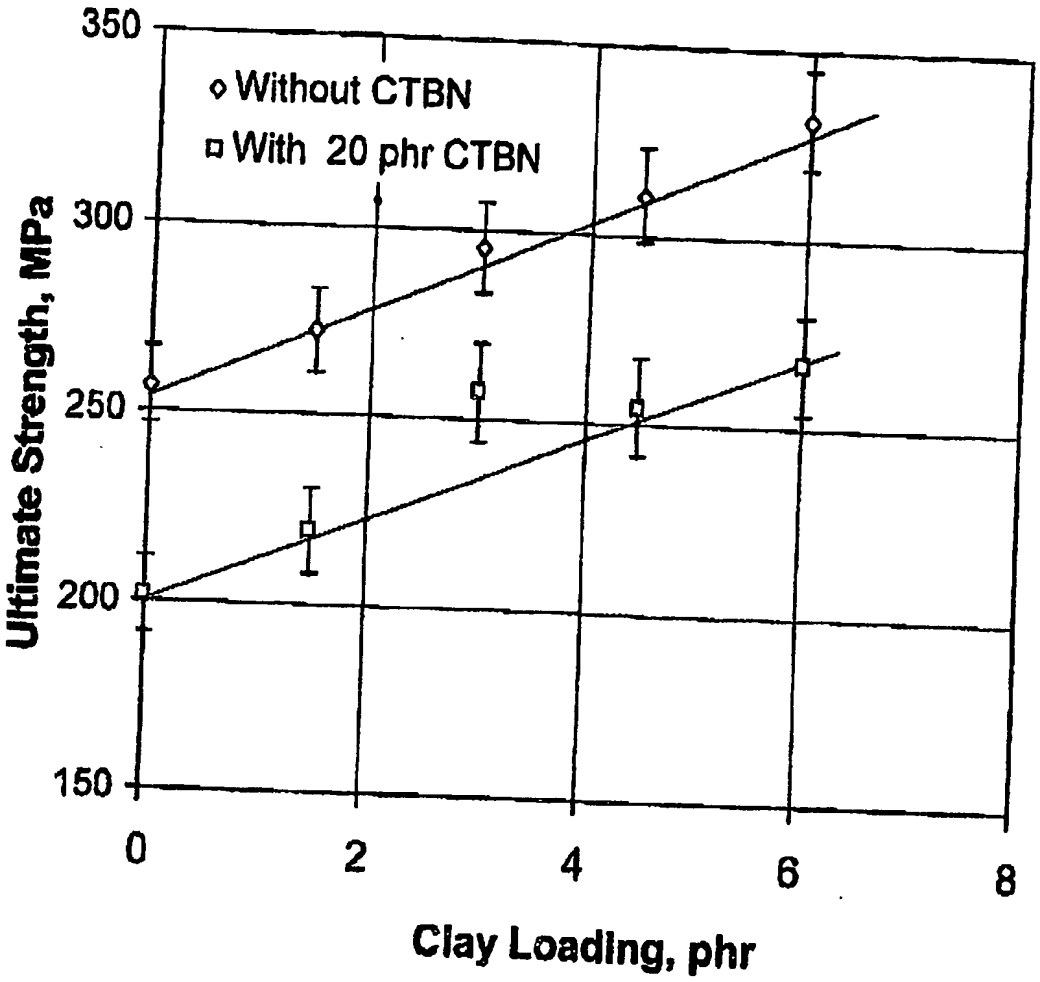
350
300
250
200
150
Without CTBN
With 20 phr CTBN
Ultimate Strength, MPa
0
2
4
6
8
Clay Loading, phr

Fig. 19

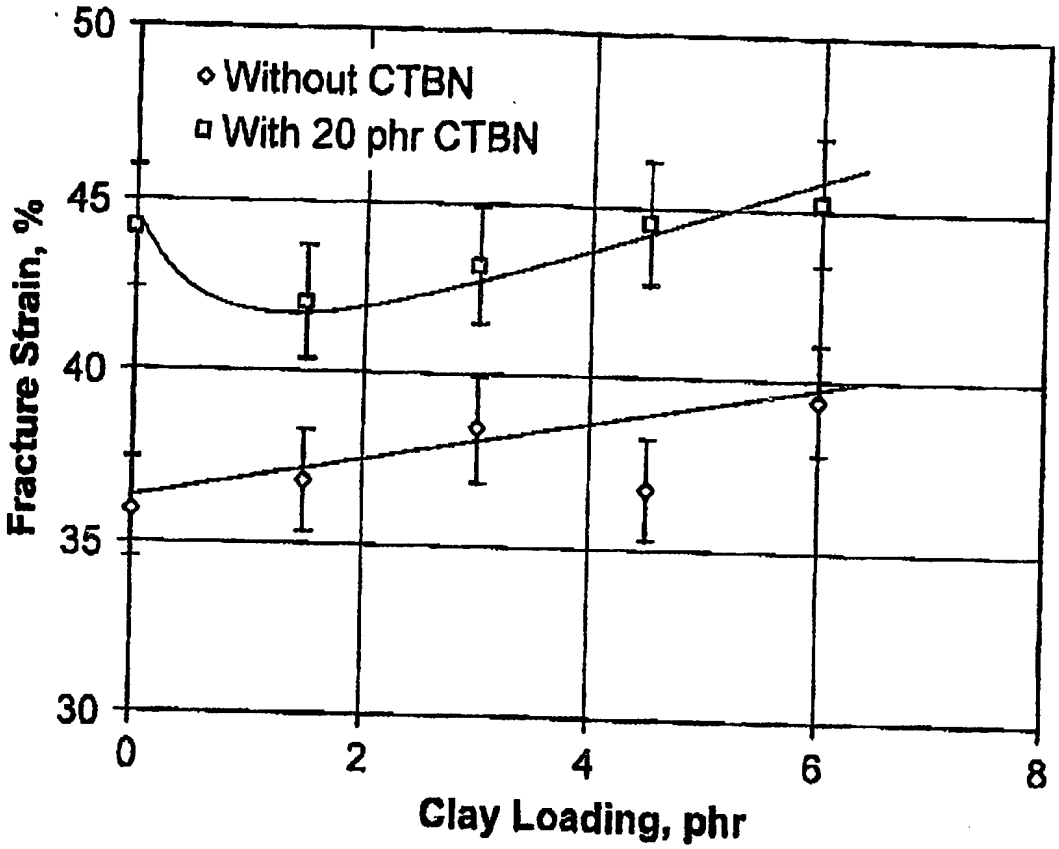
50
45
40
35
30
Without CTBN
With 20 phr CTBN
Fracture Strain, %
0
2
4
6
8
Clay Loading, phr

Fig. 20

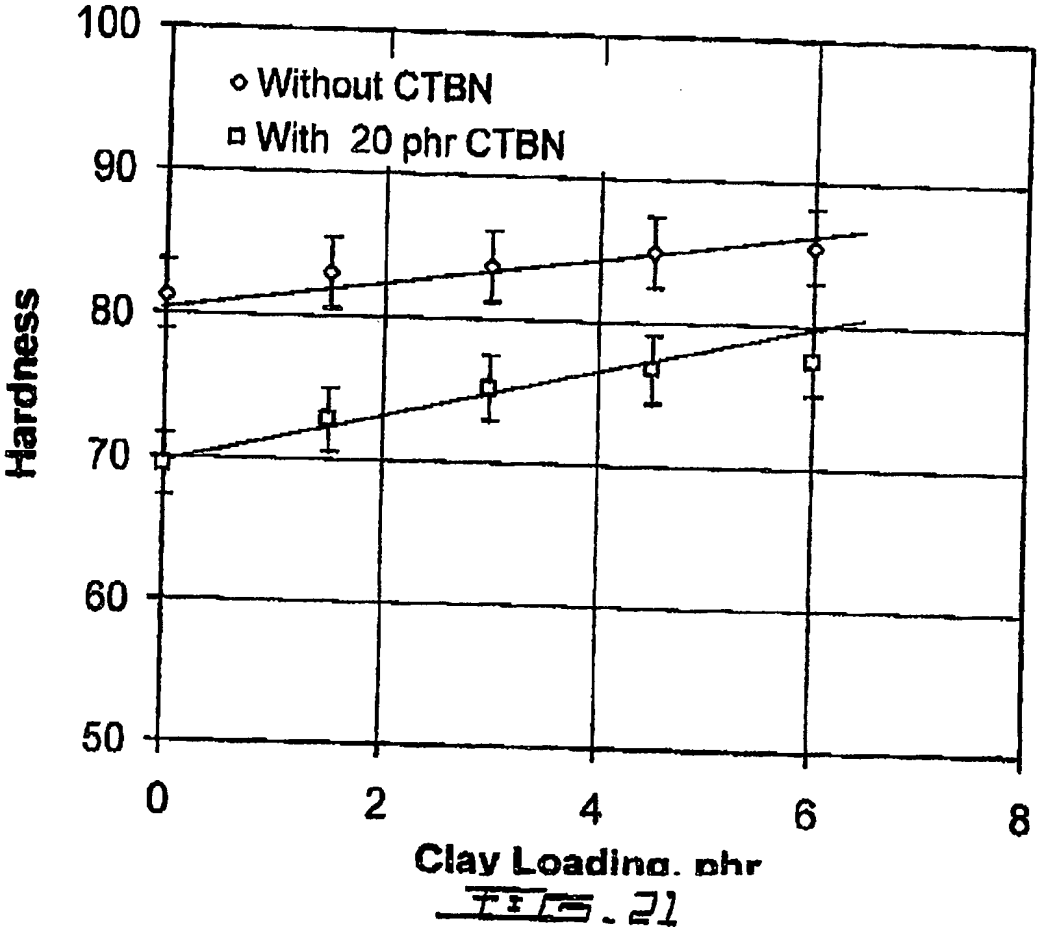
100
90
80
70
60
50
Hardness
Without CTBN
With 20 phr CTBN
0
2
4
6
8
Clay Loading, phr

FIG. 21

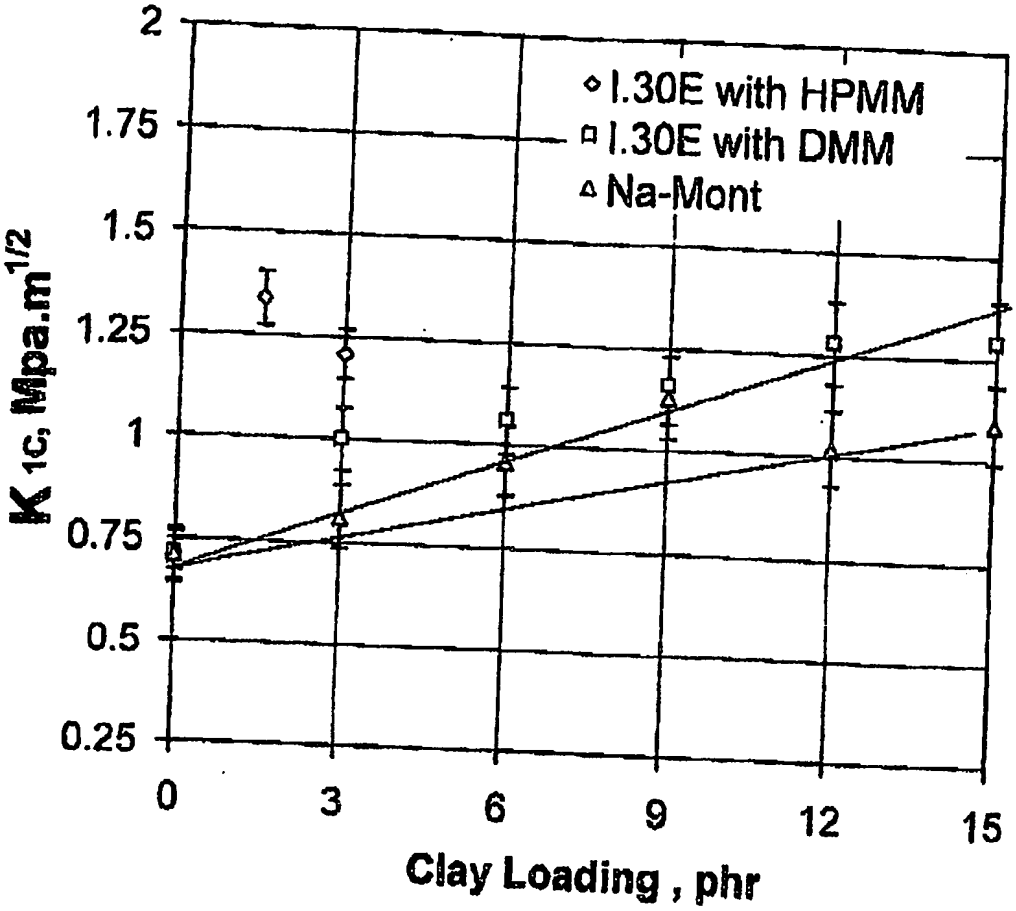
2
1.75
1.5
1.25
1
0.75
0.5
0.25
0
3
6
9
12
15
K 1C, Mpa.m1/2
Clay Loading , phr
I.30E with HPMM
I.30E with DMM
Na-Mont

Fig. 22

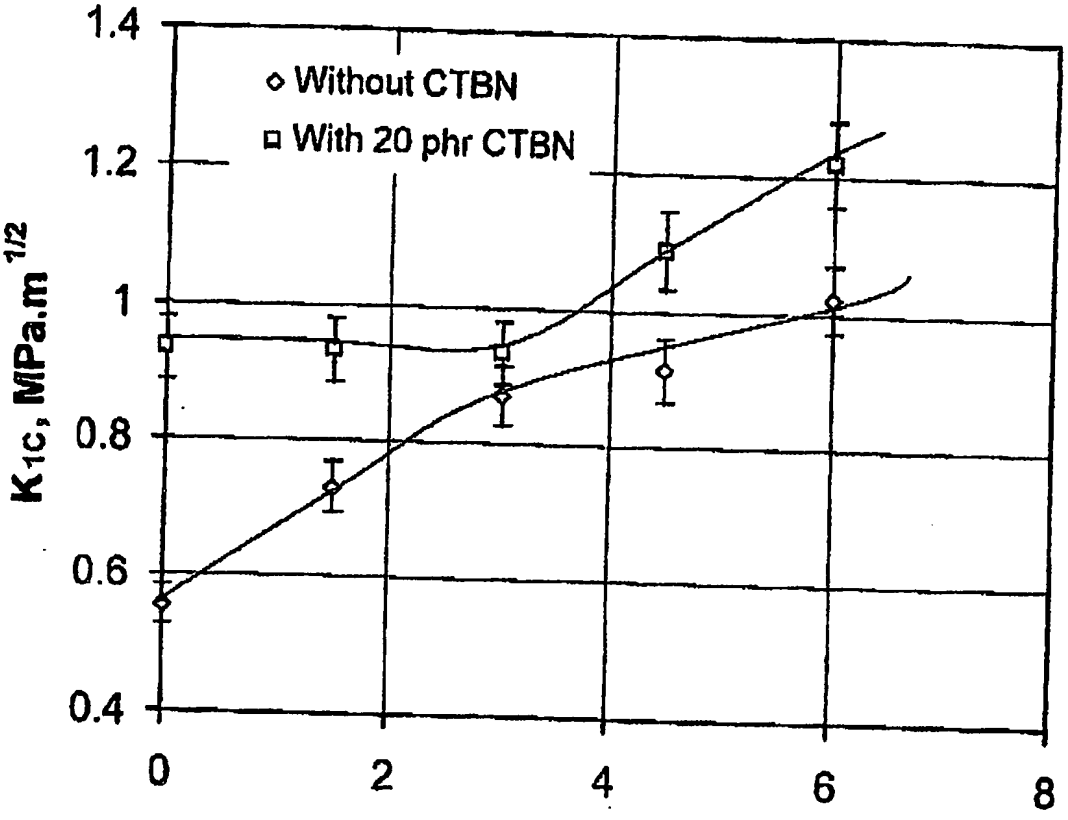
1.4
1.2
1
0.8
0.6
0.4
0
2
4
6
8
◇ Without CTBN
□ With 20 phr CTBN
K_{1C}, MPa.m$^{1/2}$
Clay Loading, phr

FIG. 23

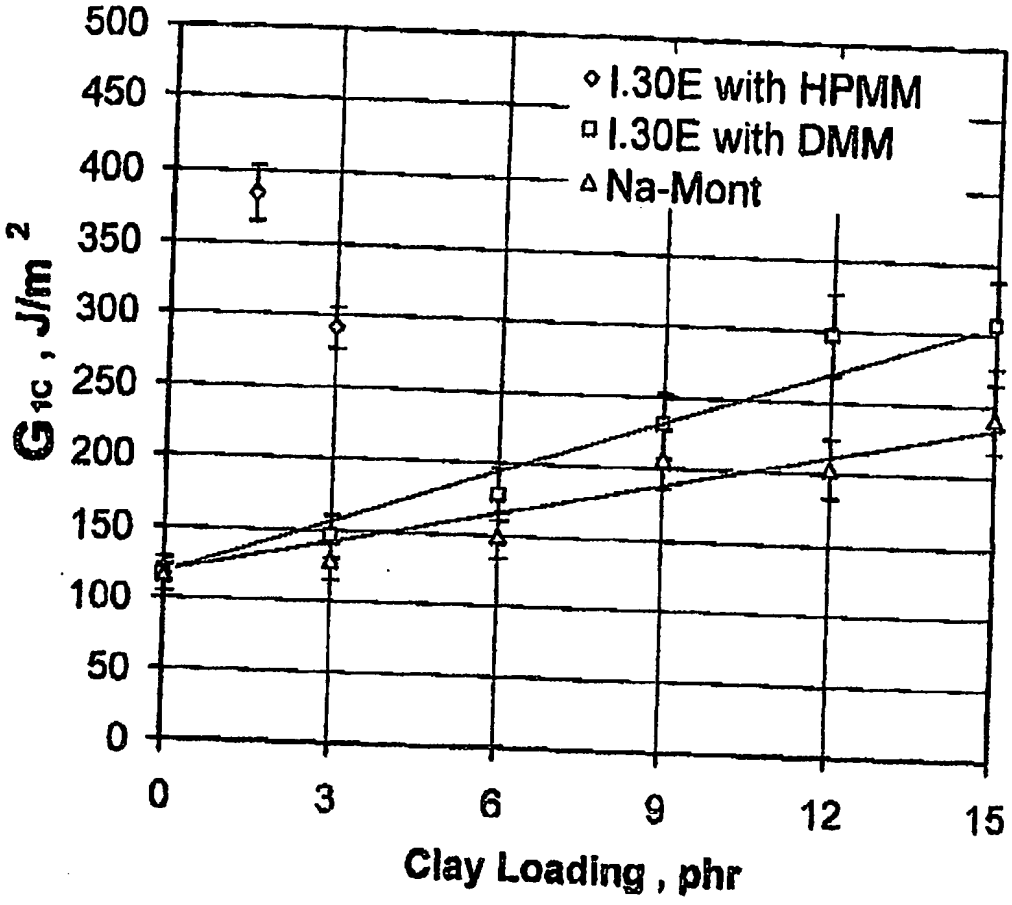
500
450
400
350
300
250
200
150
100
50
0
G_{1C} , J/m^2
0
3
6
9
12
15
Clay Loading , phr
I.30E with HPMM
I.30E with DMM
Na-Mont

Fig. 24

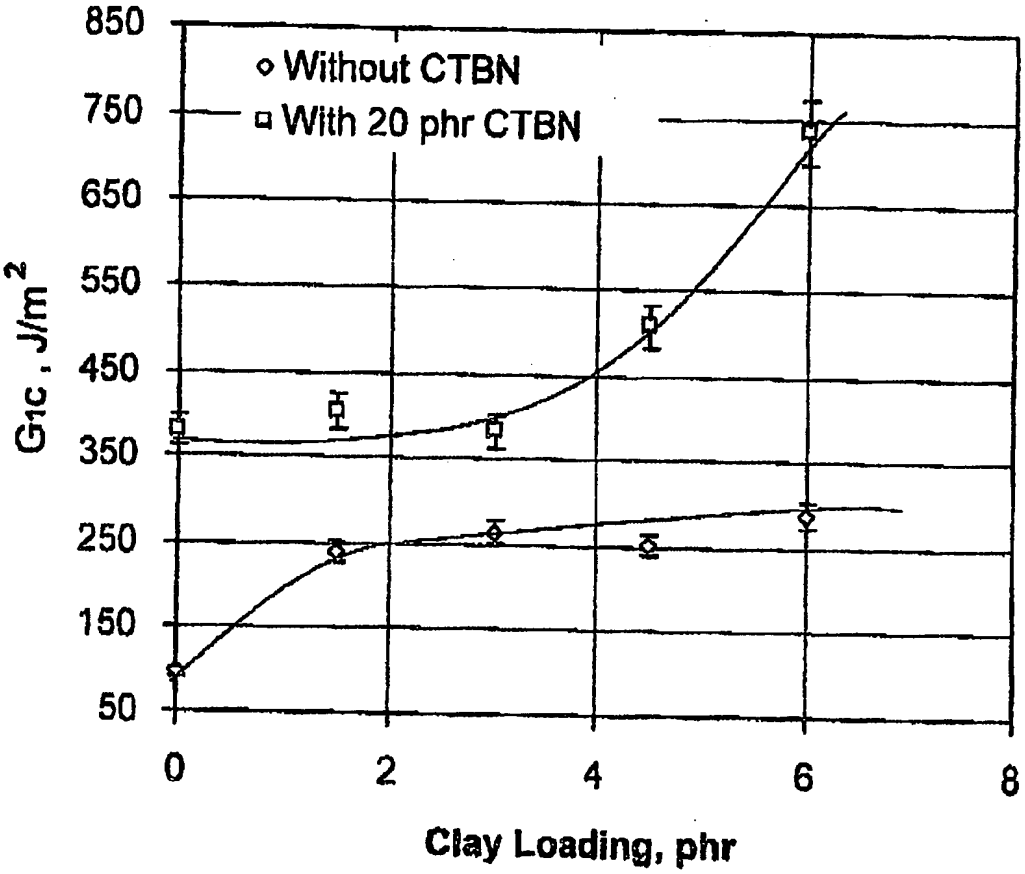
850
750
650
550
450
350
250
150
50
0
2
4
6
8
Without CTBN
With 20 phr CTBN
G1c , J/m2
Clay Loading, phr

FIG. 25

Figure 26

A

B

Figure 27

Figure 28

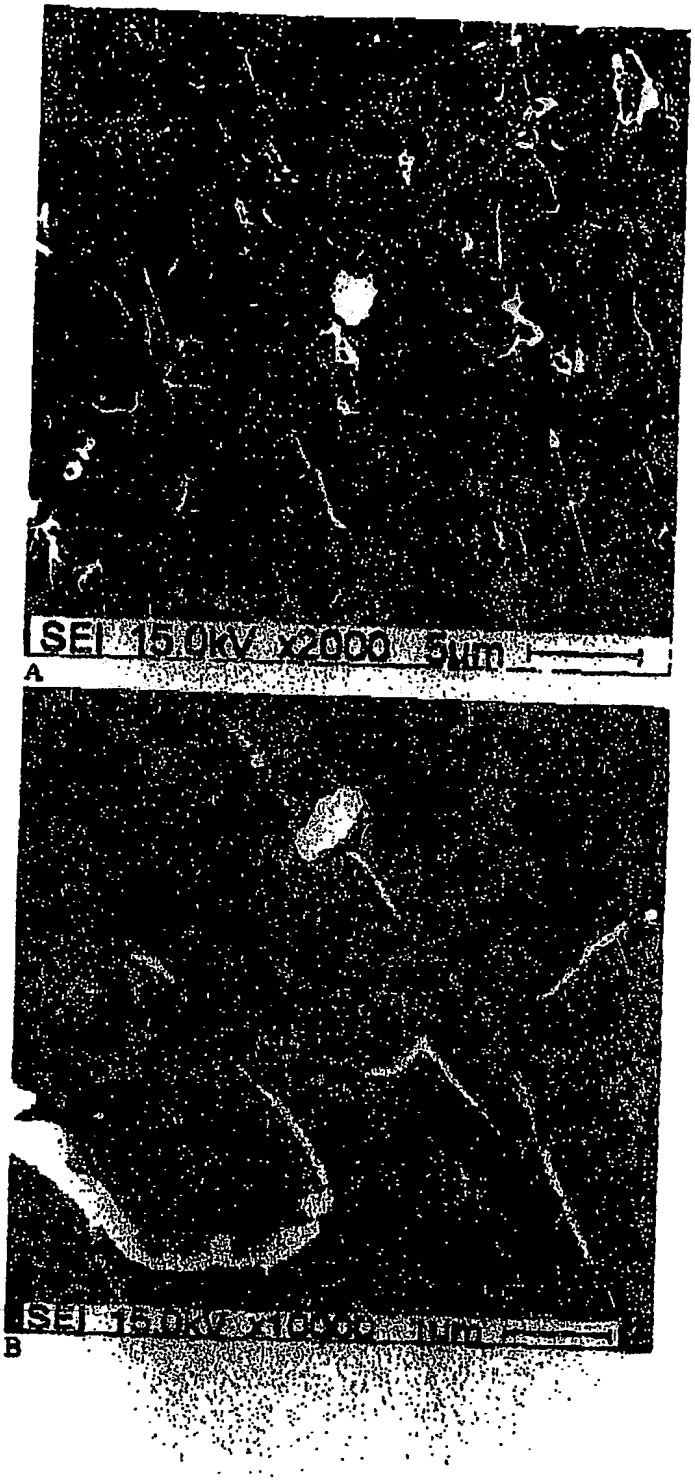

Figure 29

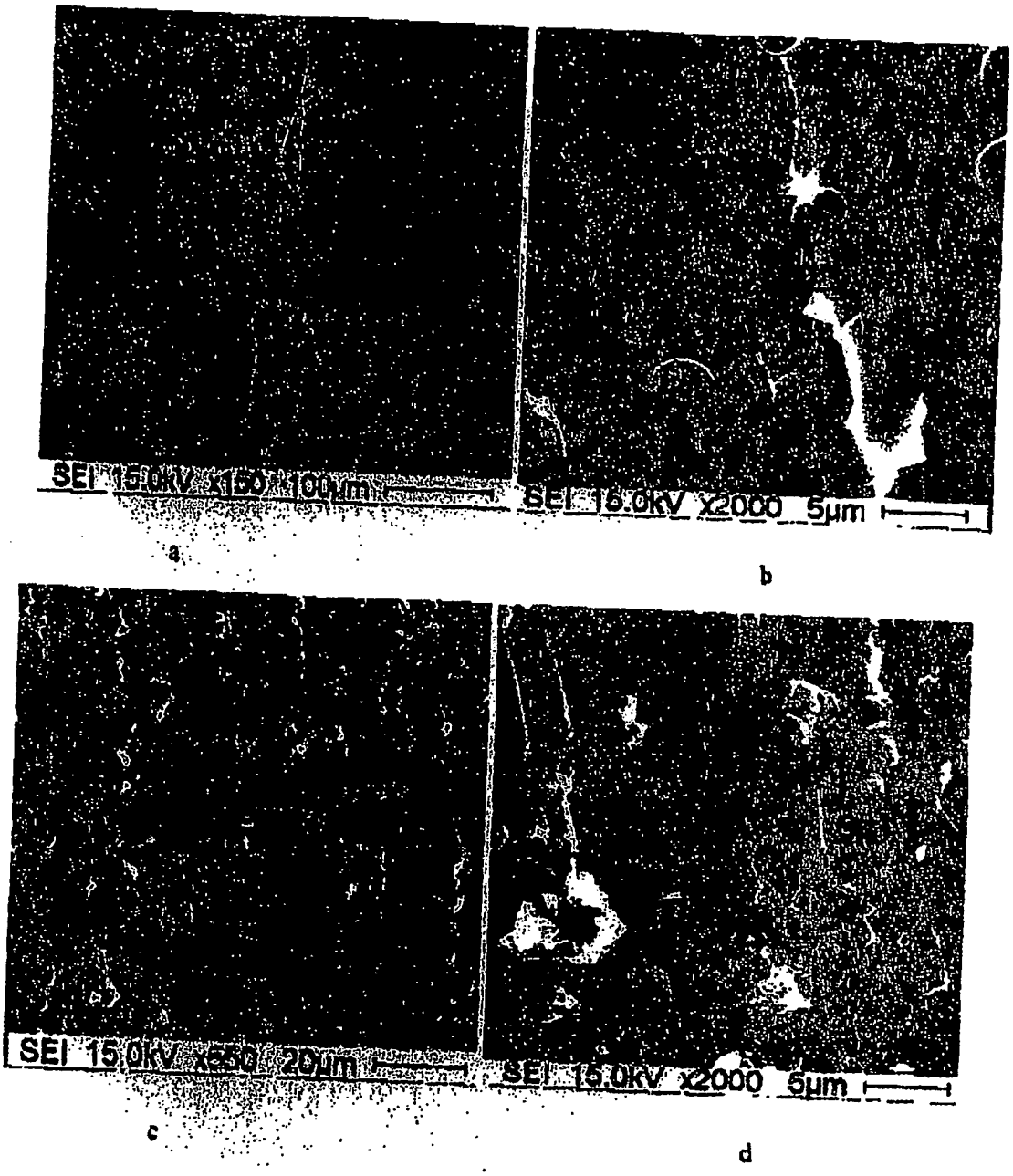
SEI 15.0kV x150 100µm
SEI 15.0kV x2000 5µm
a
b
SEI 15.0kV x350 20µm
SEI 15.0kV x2000 5µm
c
d

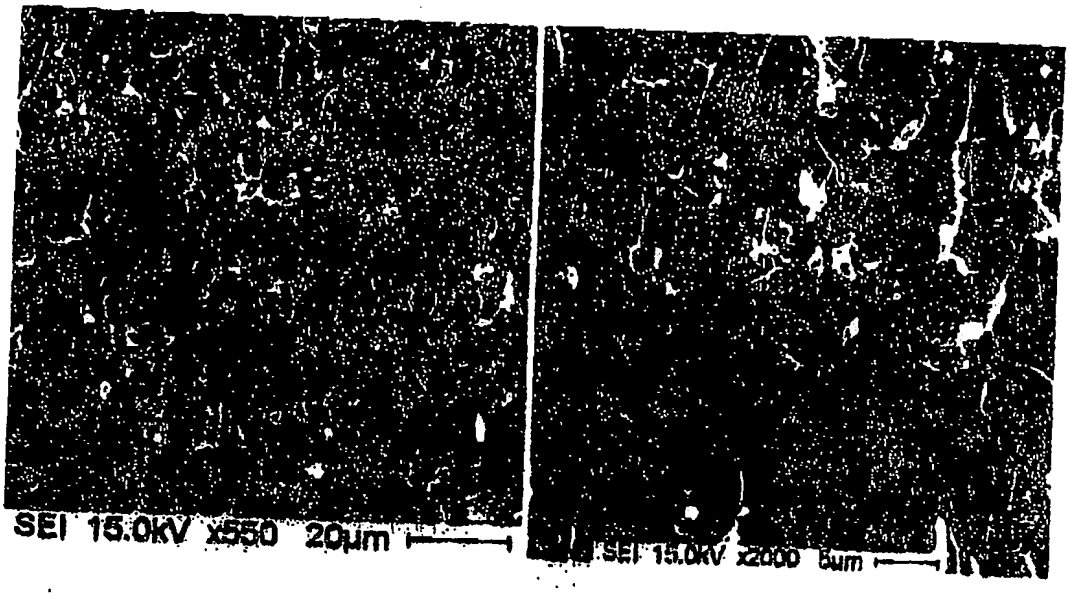
SEI 15.0kV x550 20µm
SEI 15.0kV x2000 5µm

e f

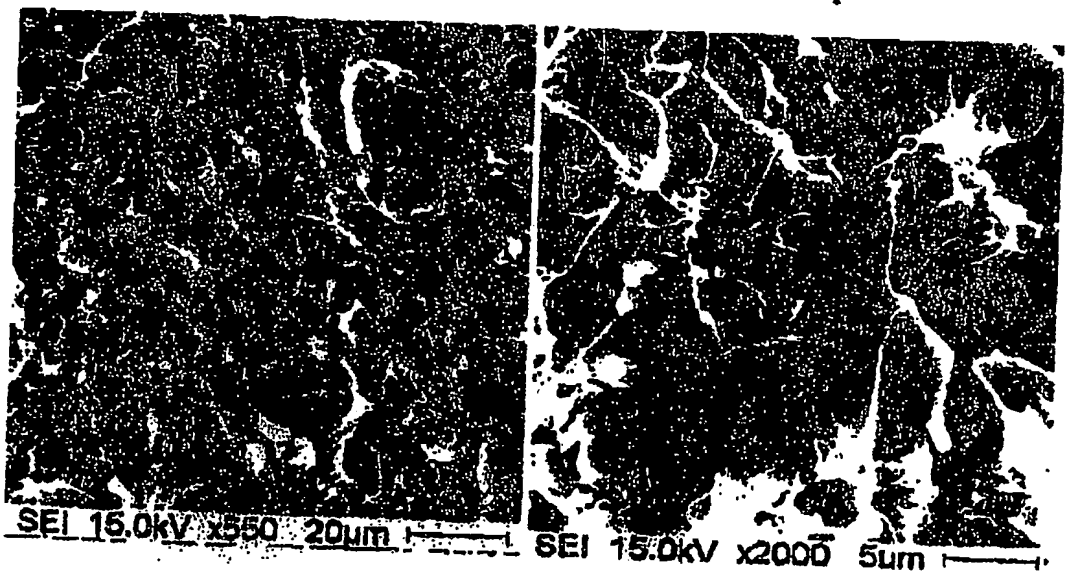
SEI 15.0kV x550 20µm
SEI 15.0kV x2000 5µm

g h

Document made available under the Patent Cooperation Treaty (PCT)

International application number: PCT/CA04/002184

International filing date: 22 December 2004 (22.12.2004)

Document type: Certified copy of priority document

Document details: Country/Office: US
Number: 60/531,618
Filing date: 23 December 2003 (23.12.2003)

Date of receipt at the International Bureau: 30 March 2005 (30.03.2005)

Remark: Priority document submitted or transmitted to the International Bureau in compliance with Rule 17.1(a) or (b)

World Intellectual Property Organization (WIPO) - Geneva, Switzerland
Organisation Mondiale de la Propriété Intellectuelle (OMPI) - Genève, Suisse